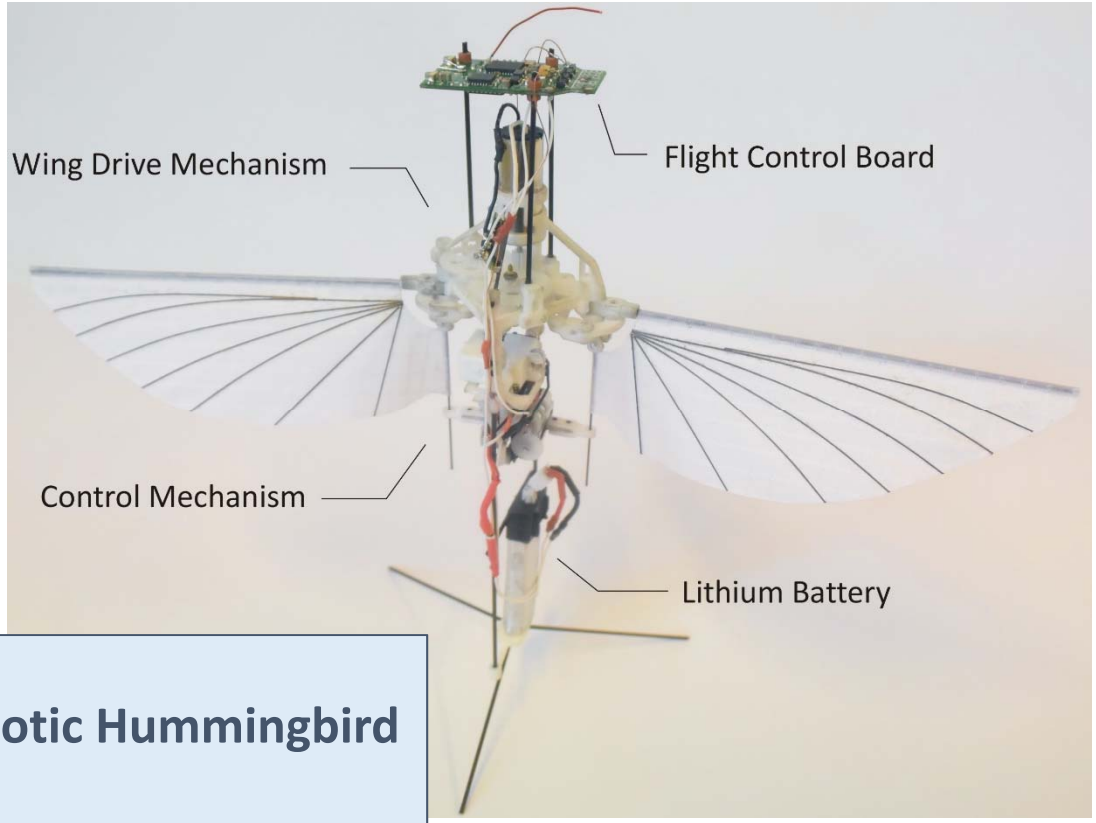

COLIBRI: A Robotic Hummingbird

André Preumont & Ali Roshanbin
Université Libre de Bruxelles (ULB)

GT-UAV
Compiègne
12-10-2018

Contents

Hummingbird aerodynamics
Tailless hovering flapping twin-wing UAVs
Colibri project
- Flapping mechanism
- Wing design
- Aeroelasticity
- Attitude control moments
- Dynamics and control
- Attitude stabilization (pitch-roll)
- Flight tests
- Drift speed control
- Future work

NATURE - Hummingbirds: Magic in the Air
http://www.youtube.com/watch?v=Hrlr45uGapQ

Aerodynamics of the hovering flight

2-D wing

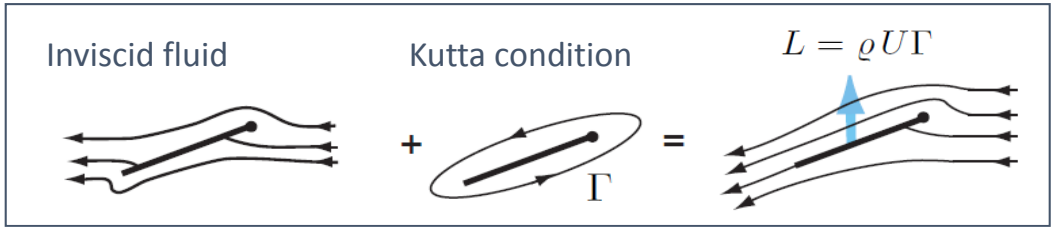

Simplified vortex patterns of a bird in steady flight
(U.M. Lindhe Norberg)

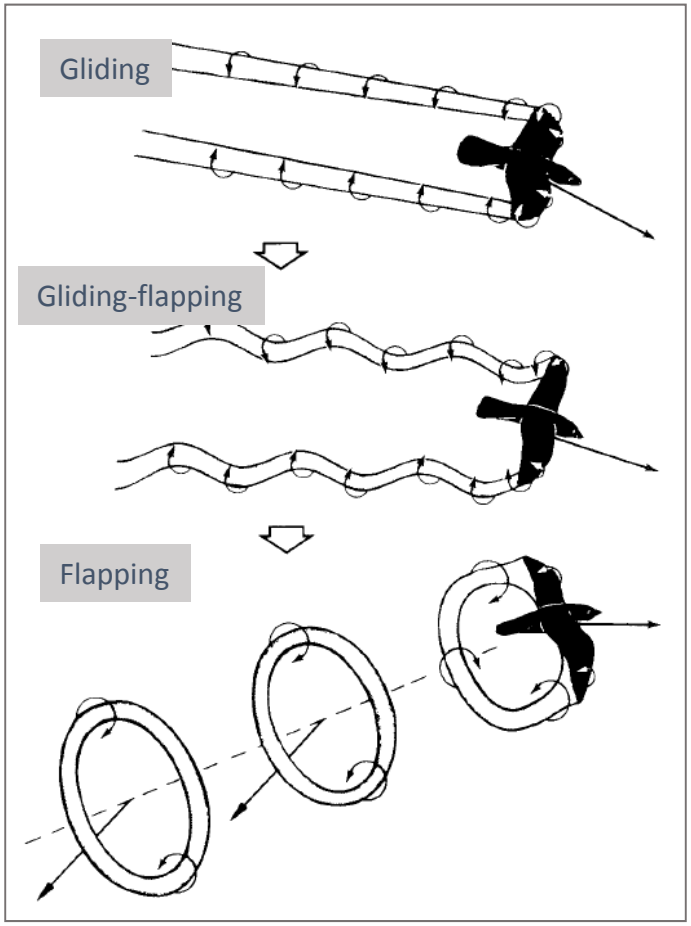

Hovering (CFD simulation Song et al., 2014)

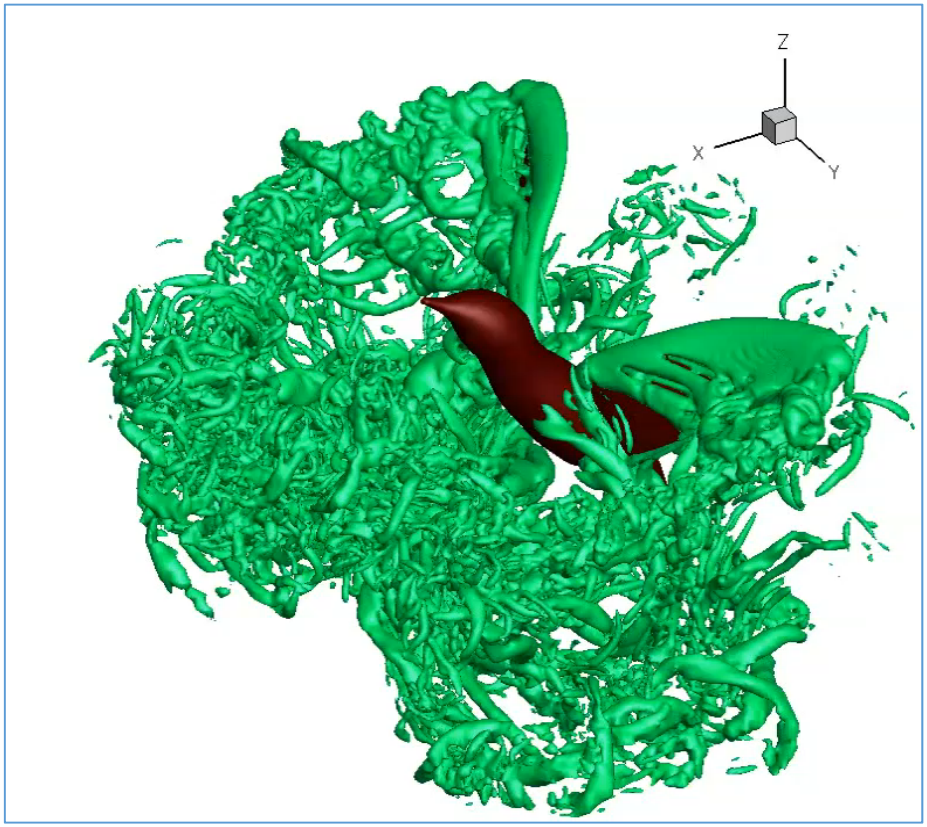

Hummingbird wing tip trajectory in hover

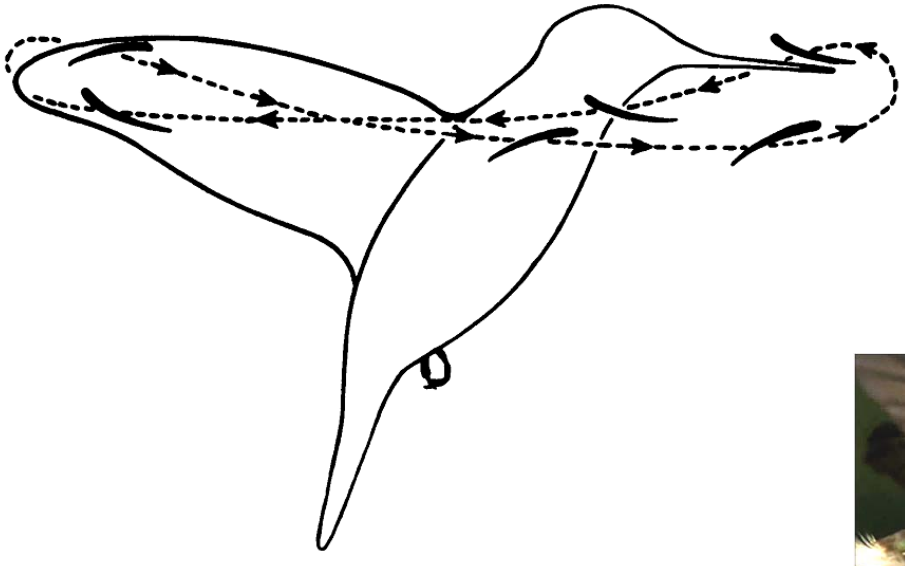

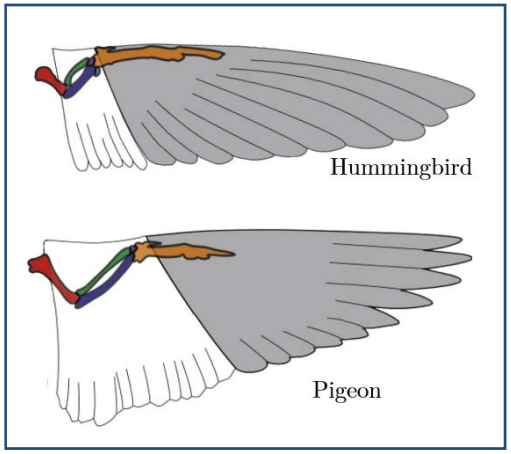

Bats have the capability to **actively control the camber** with their fingers to delay stall

Common fruit bat (Wikipedia)

Townsend's big ear bat (Wikipedia)

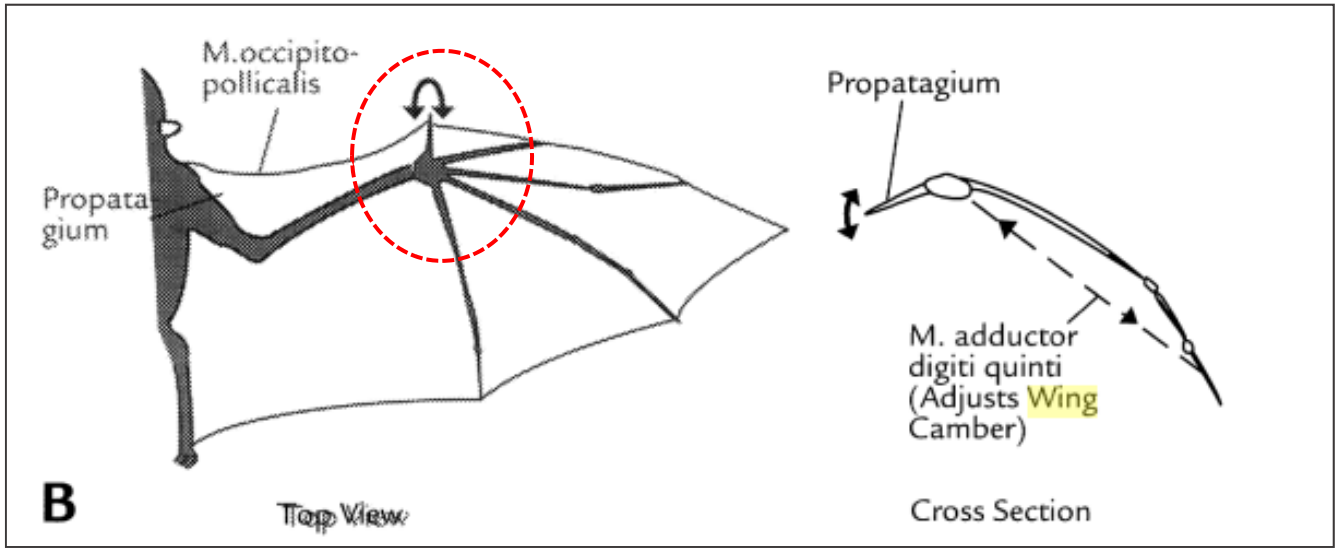

(G. Neuweiler)

Flapping twin-wing robots

KUBeetle
Konkuk University Korea
15.6 cm wing span
21.4 g, 30 Hz

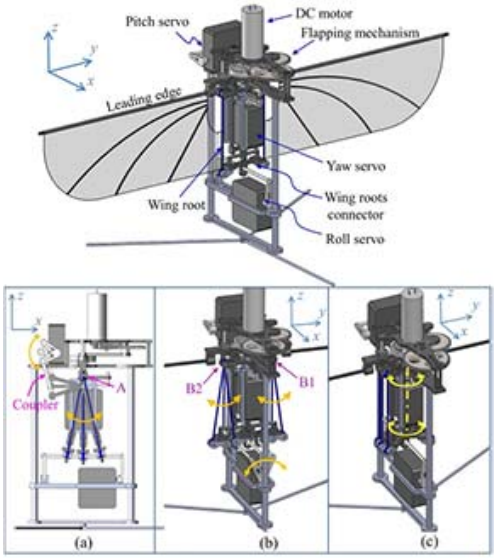

DARPA-AeroVironment
Nano Hummingbird
16,5 cm wing span
19 g, 30 Hz

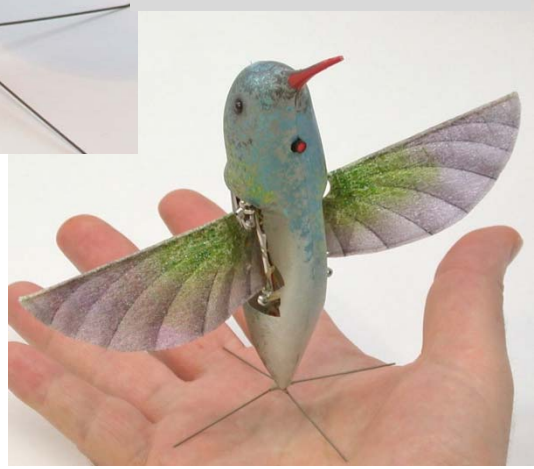

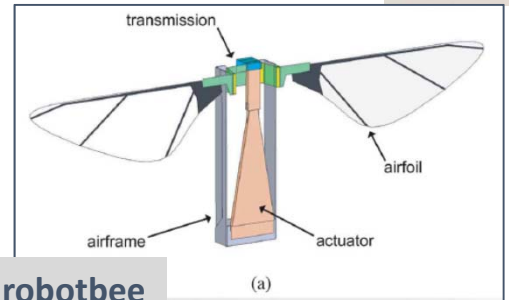

Harvard robotbee
3.5 cm wing span
80 mg, 120 Hz

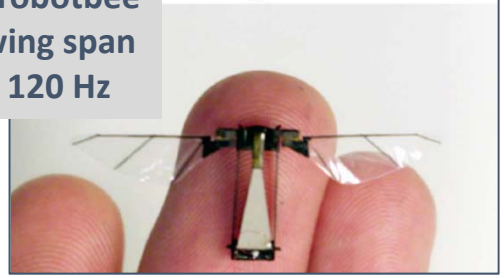

Nano Hummingbird
Developed by AeroVironment Inc. (5 years)
Financed by DARPA (UD$: 4 million)

Comparison between robotic and living hummingbirds

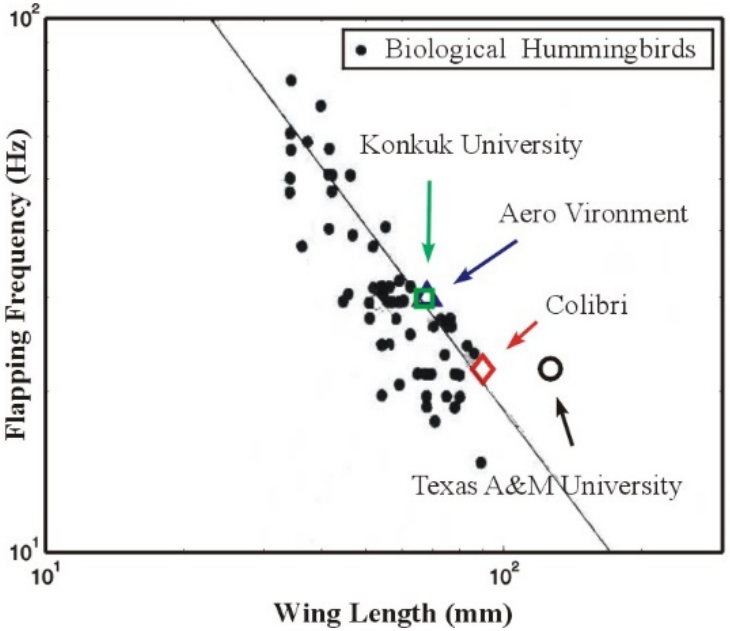

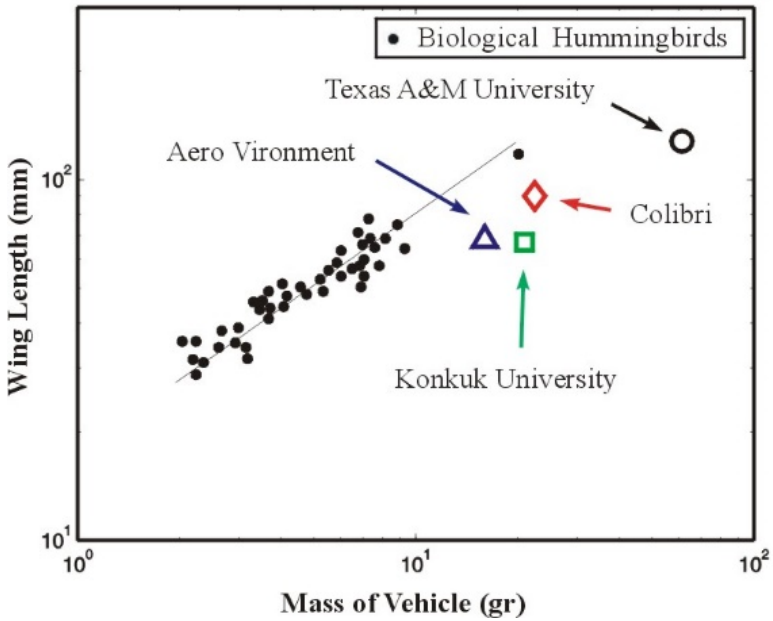

(adapted from Greenwalt)

Flapping Mechanism

Slider-crank and four-bar mechanism

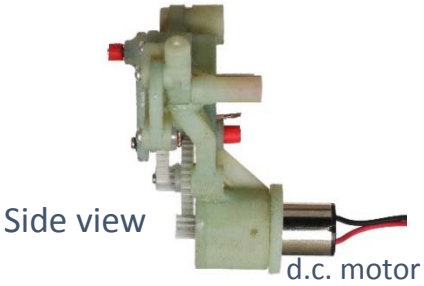

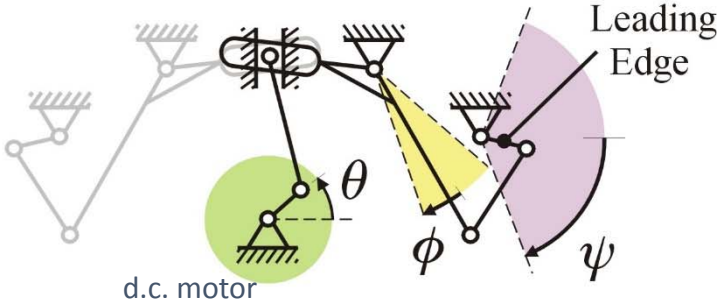

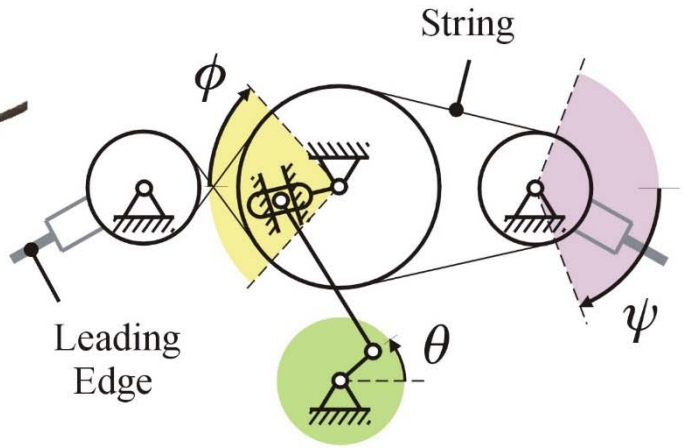

- More symmetrical
- Less backlash

String-based mechanism

String based mechanism vs. Four-bar mechanism
Less backlash – More symmetrical

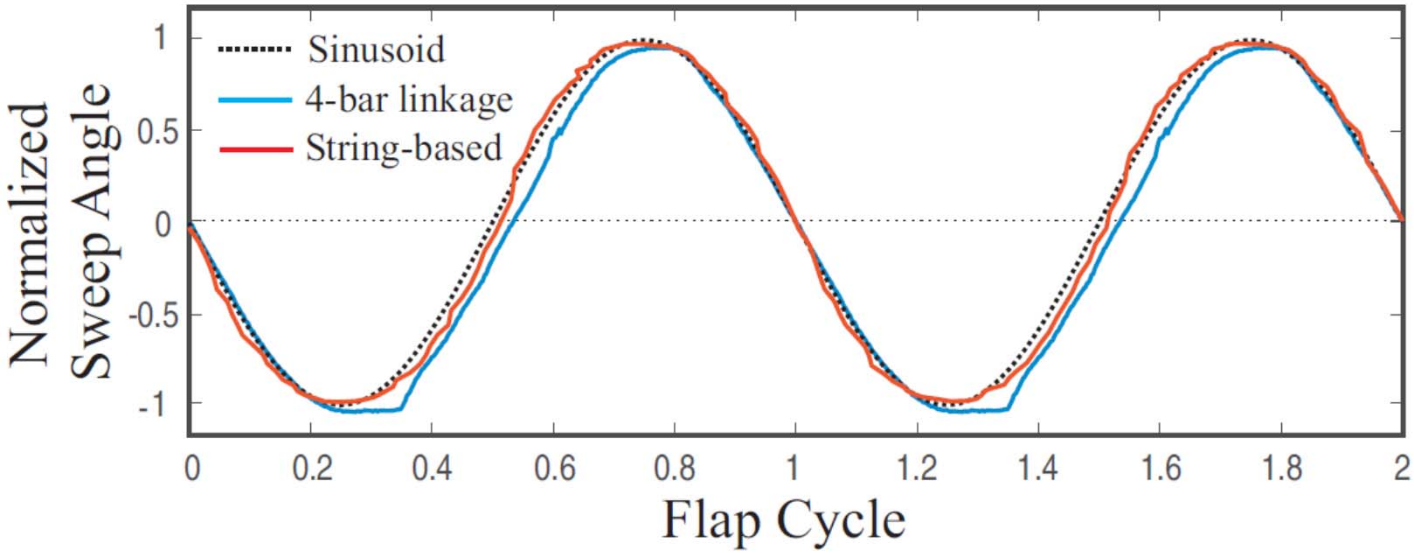

Fig. 6. Comparison of the wing kinematic profiles (measured at the root of the shoulder) of the four-bar and string-based flappers. The experiment is performed at the frequency of 1 Hz to remove dynamical loads. The vertical axis (sweep angle) is normalized.

Exploded view of the **flapping mechanism**
(string-based) 3D printing Nylon PA2200

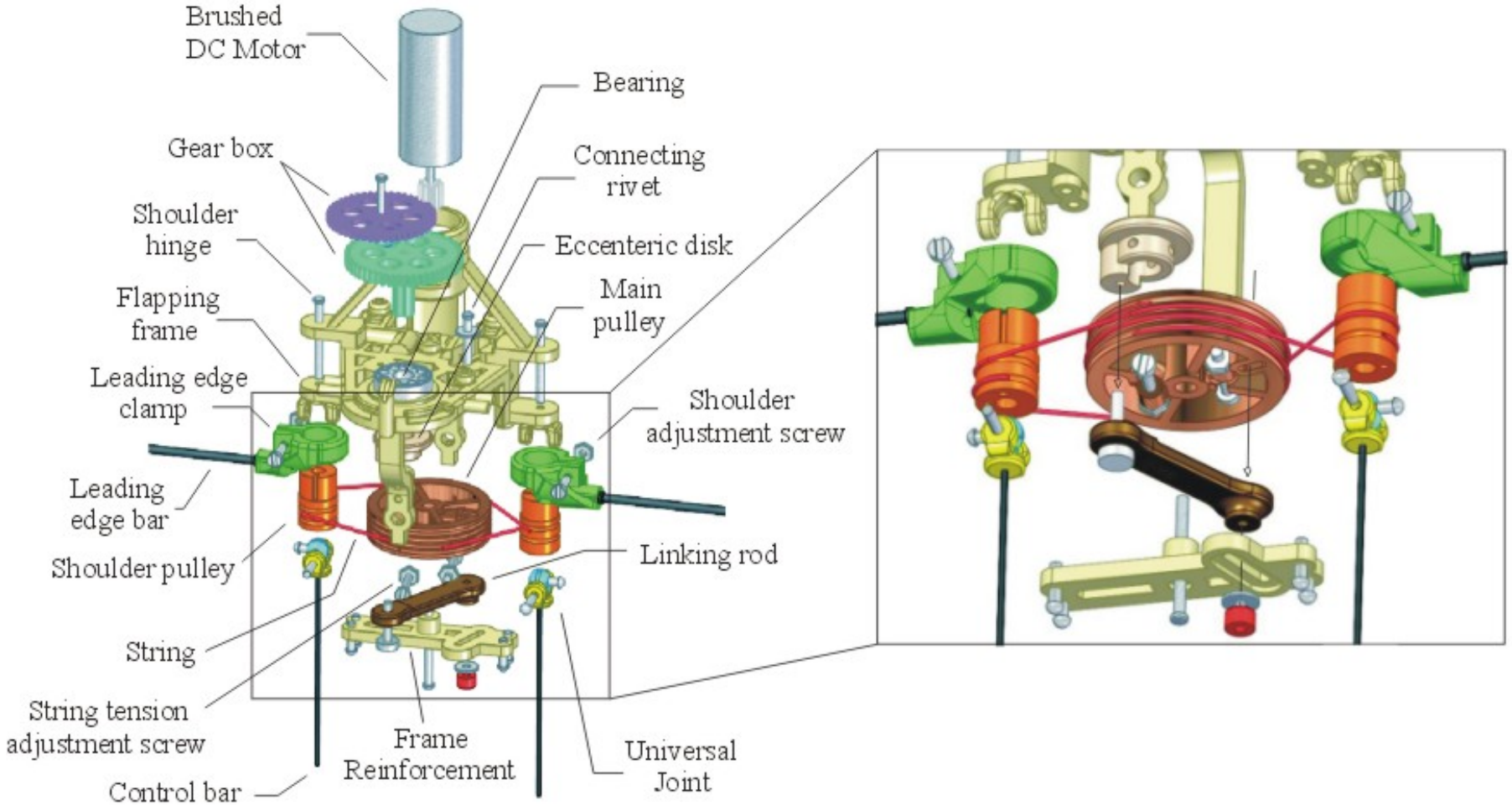

Wing Aerodynamics: Membrane wings with passive camber

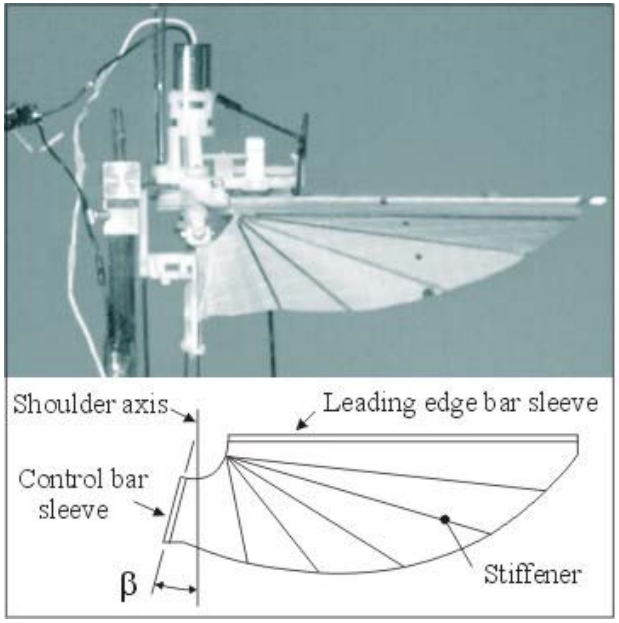

Various wing shapes used in the project

The wing camber is obtained passively as a result of aerodynamic forces, thanks to the Camber angle β

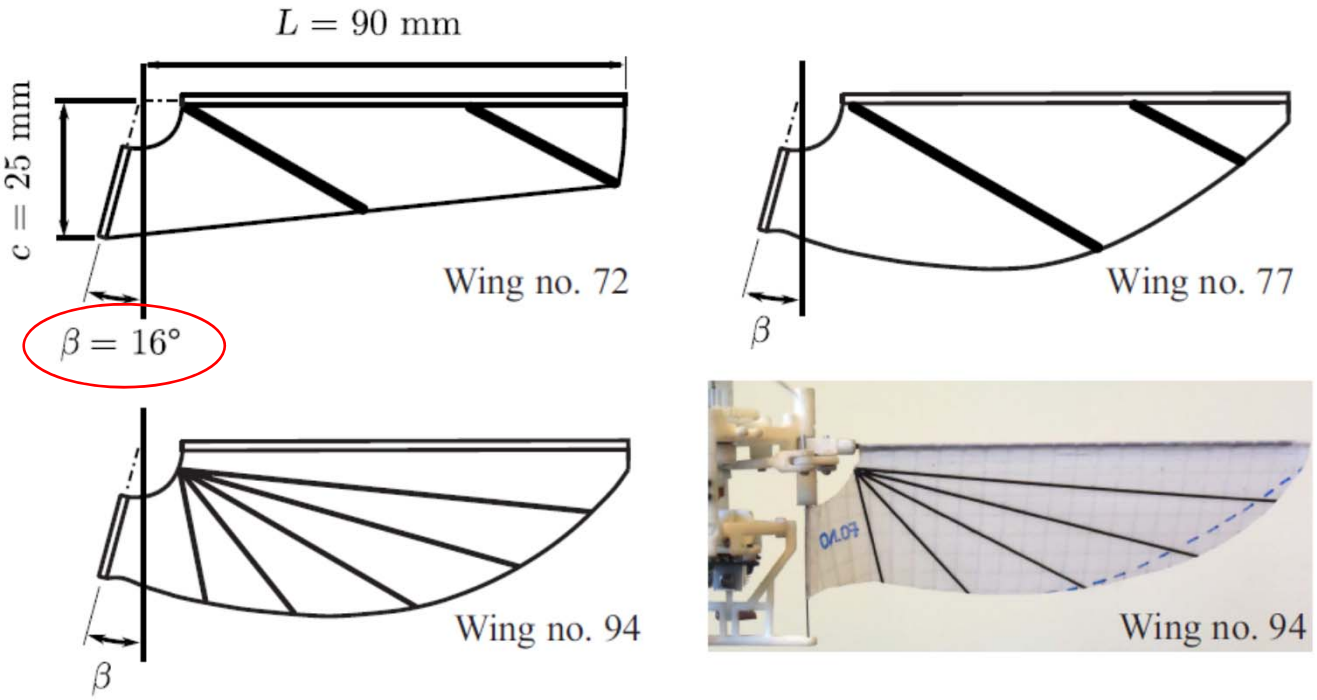

Hot wire anemometer air flow measurements of the downwash air velocity in the plane below the robot

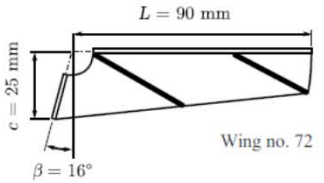

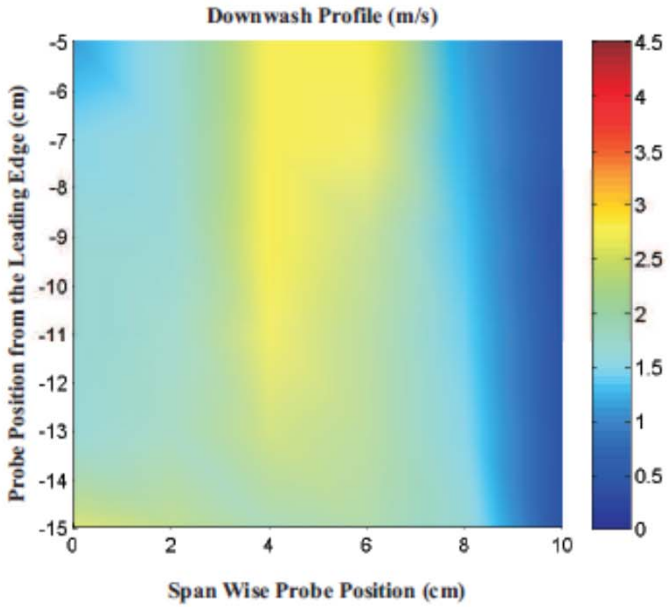

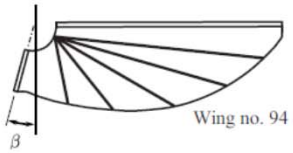

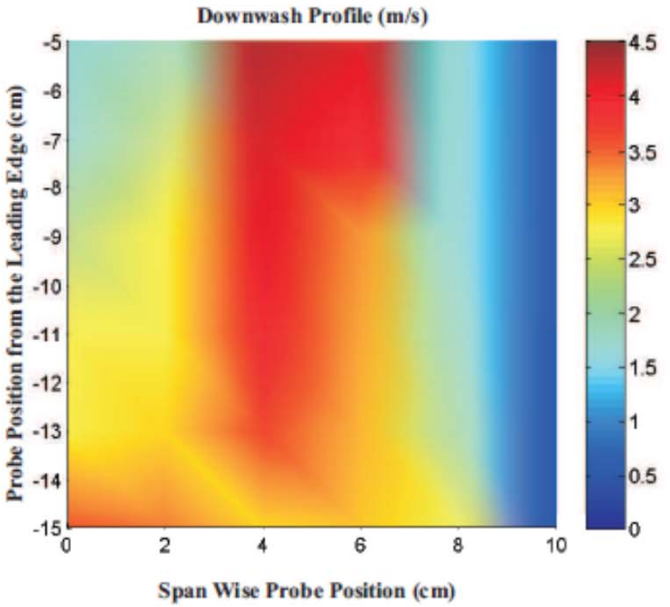

Lift vs. Frequency measurements of wings 72 and 94 (1 mm leading edge bar)

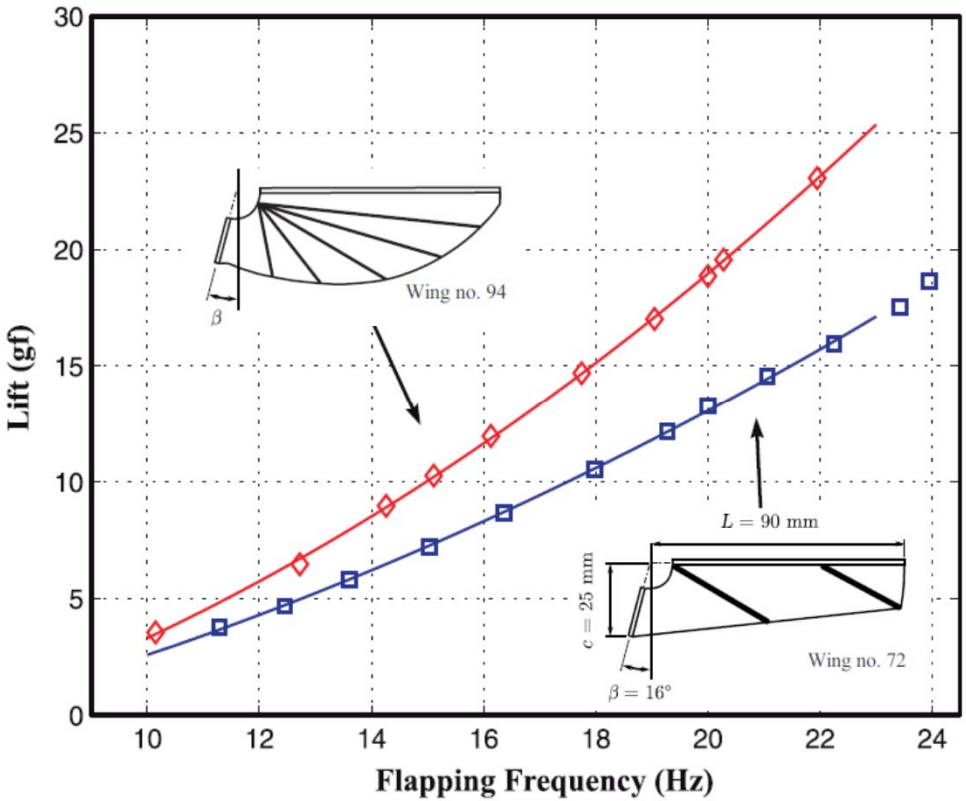

Wing tip trajectory d=0.7 mm

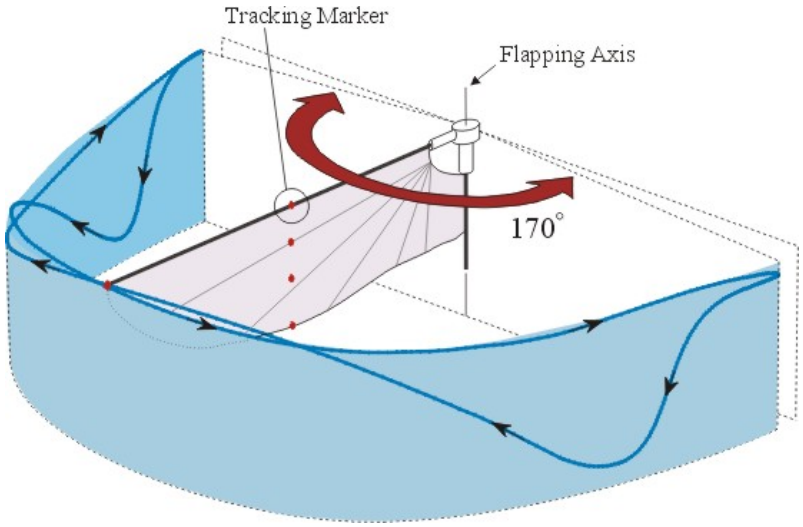

Wing rotation angle

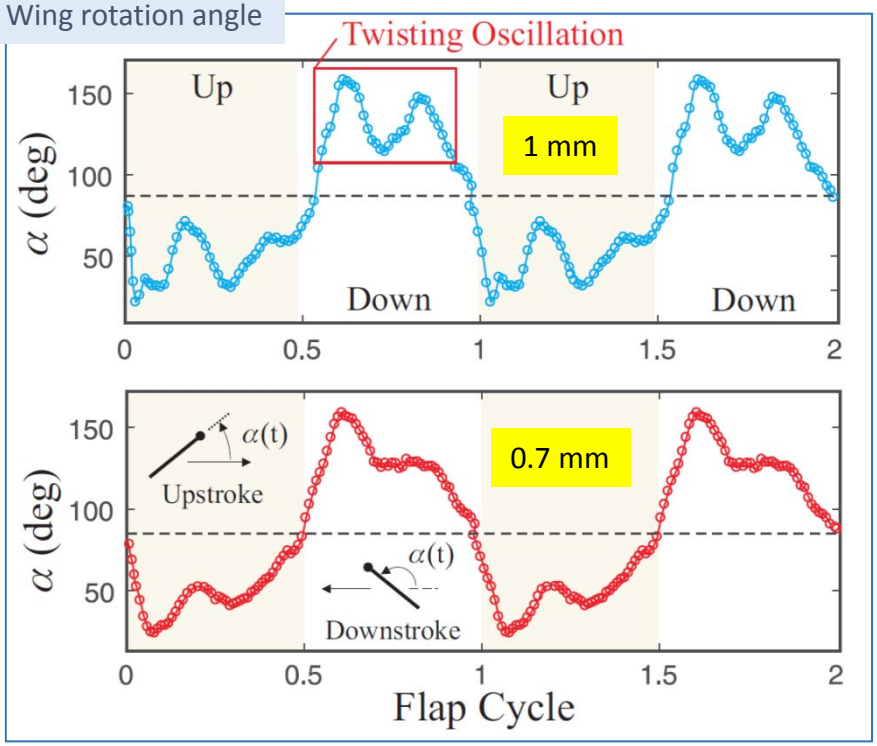

Aeroelasticity

Taking advantage of the leading edge bar flexibility

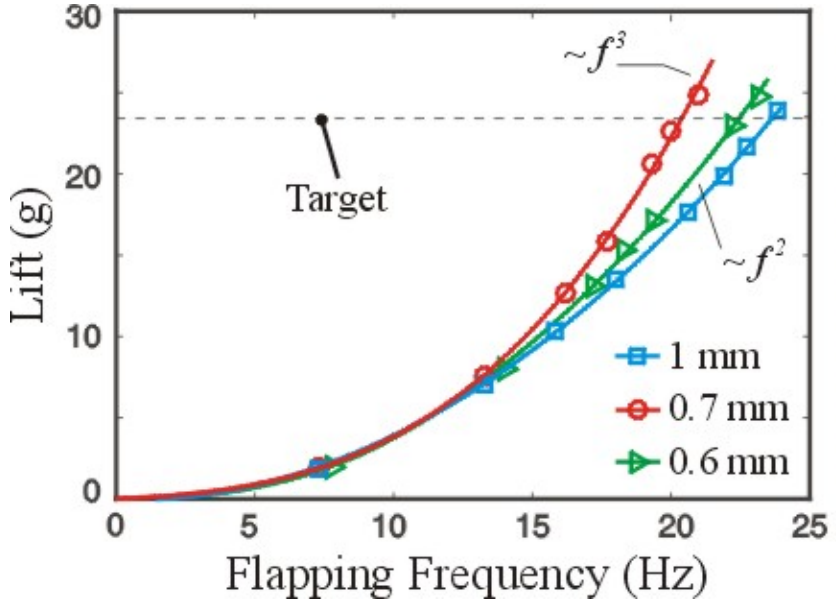

Aeroelasticity

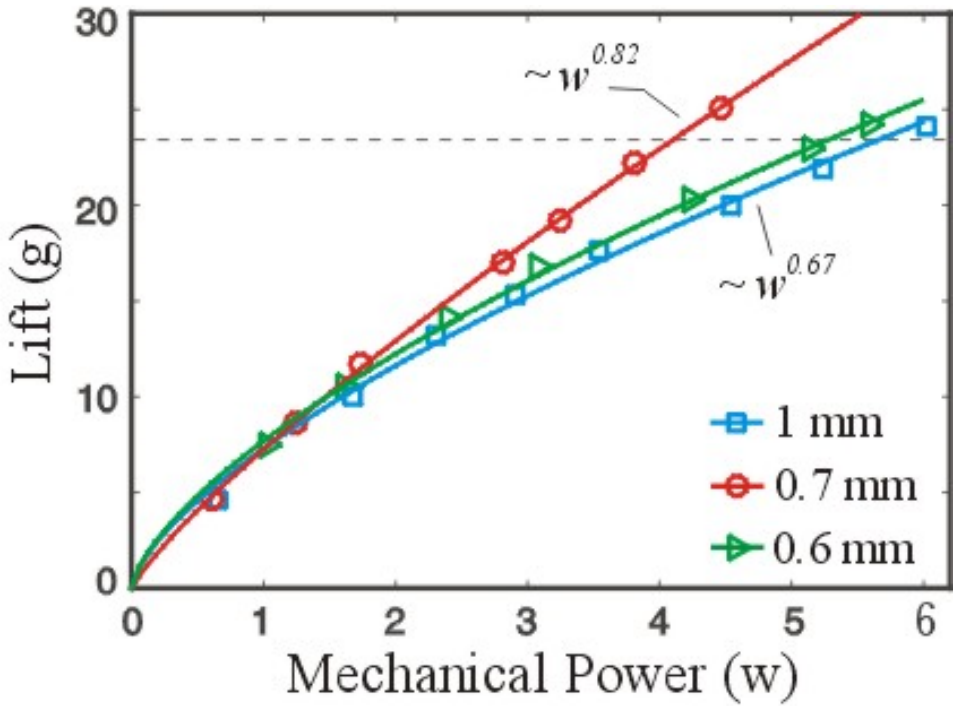

With leading edge carbon bars of 0.7 mm, **specific mechanical power: 170 W/kg**
(Specific aerodynamic power of *Calypte anna* hummingbird: 130 W/kg)

Lift versus Electrical power
Comparison with propellers of comparable size

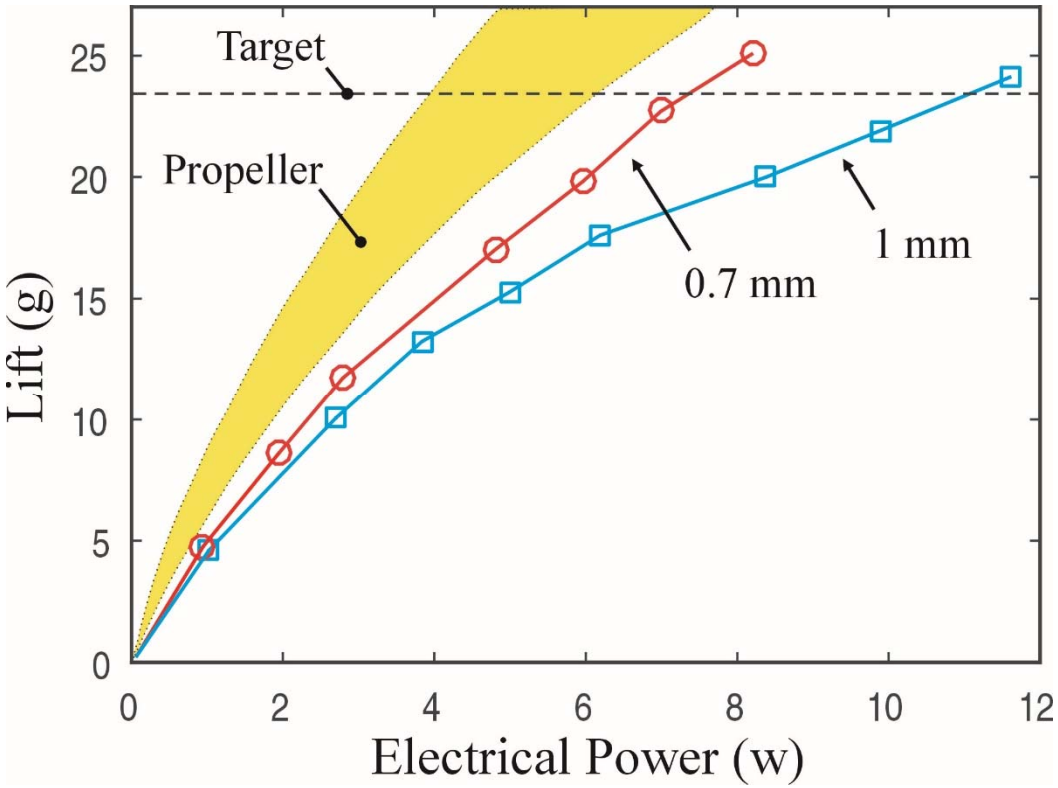

More flexible leading edge bars reduce sensor noise

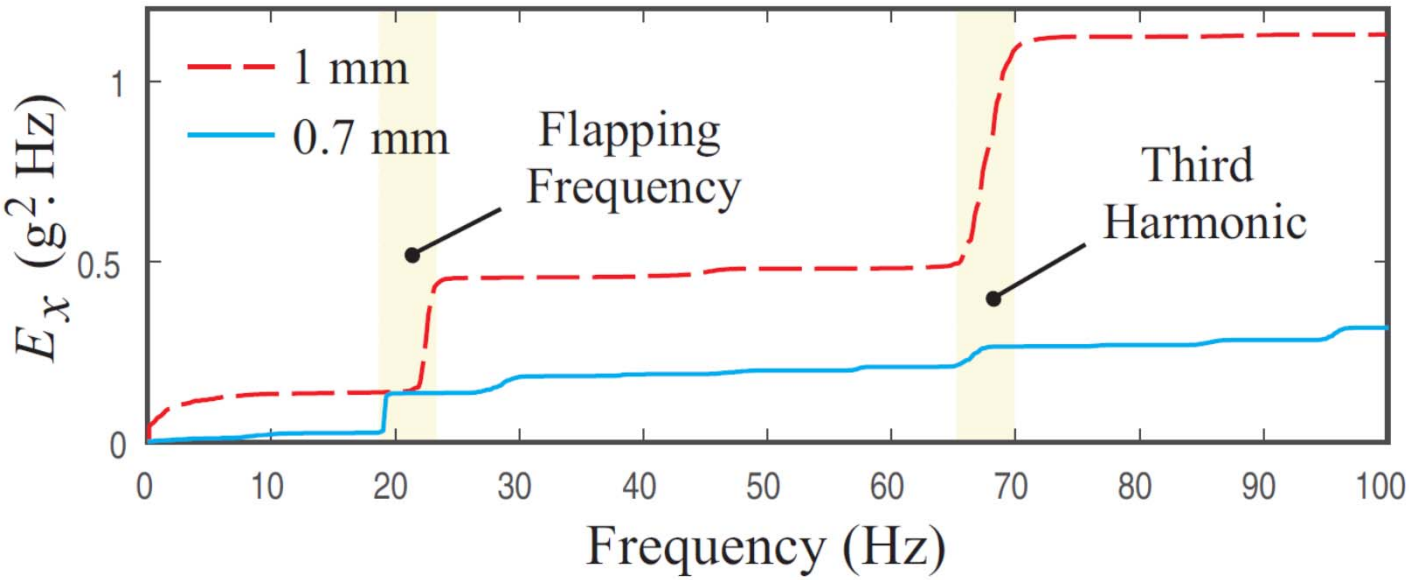

Fig. 8. Effect of the leading edge bar diameter of the string-based mechanism on the cumulative energy in the linear axial (front-back) acceleration signal measured by the on-board inertial sensor at hovering.

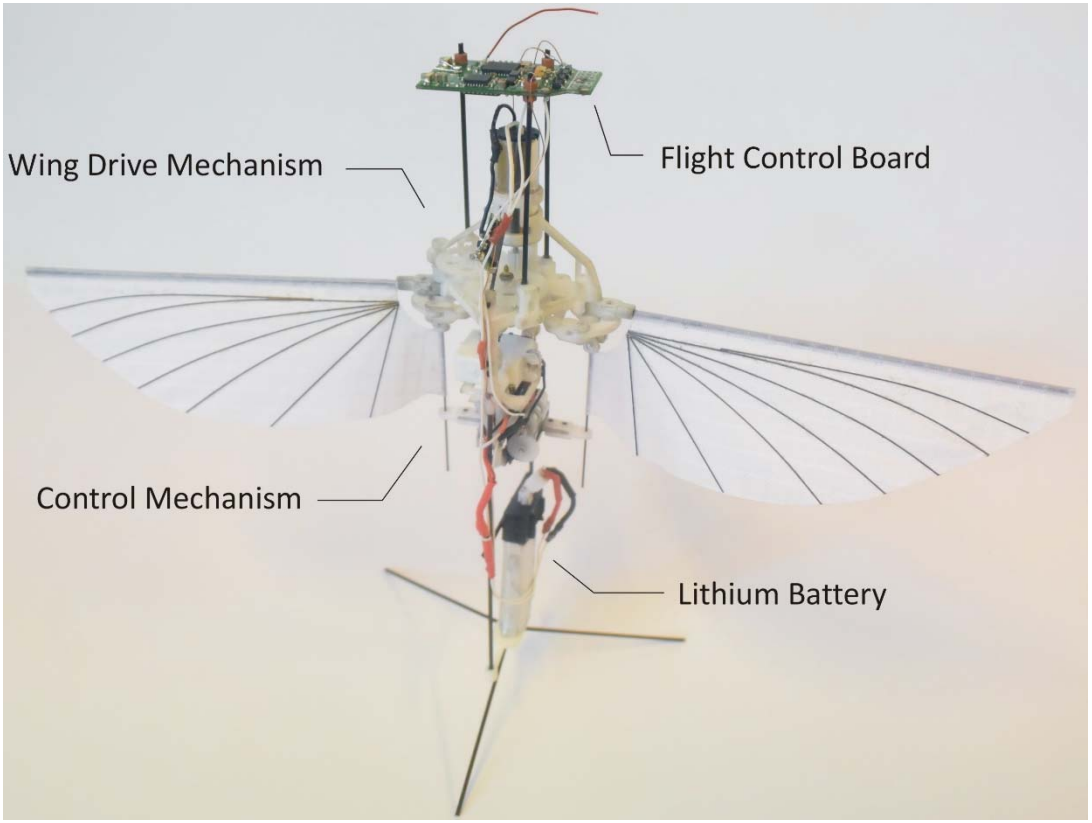

COLIBRI weight distribution

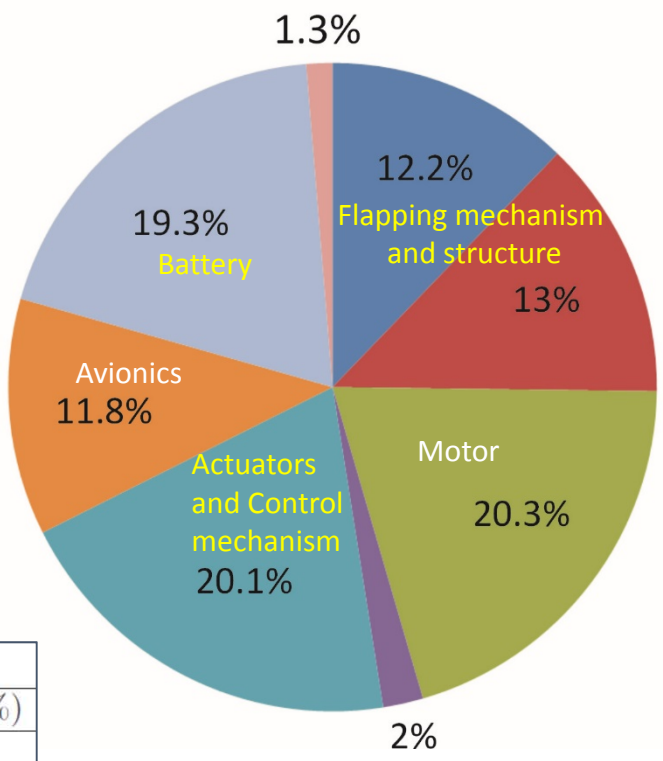

Table 1: Colibri Weight Breakdown		
Component	Weight (gr)	Percentage of Total (%)
Flapping mechanism + Structure	6	25.2
Motor (EPS8-Brushed DC)	4.85	20.3
Wings (Icarex + carbon)	0.48	2
Control mechanism + Actuators	4.8	20.1
Avionics (Micro MWC multiwii)	2.12	8.9
Bluetooth	0.7	2.9
Wiring+connectors	0.3	1.3
Battery	4.6	19.3
Total	23.85	100

Attitude control actuation
Wing twist modulation mechanism
[Keennon et al.]

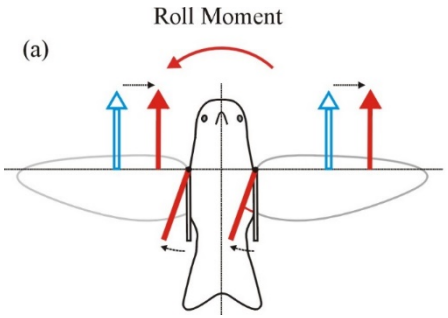

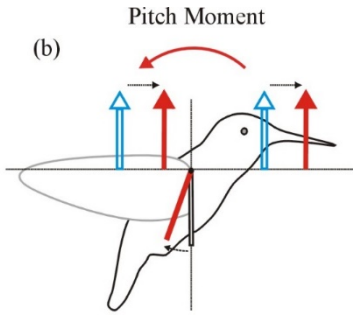

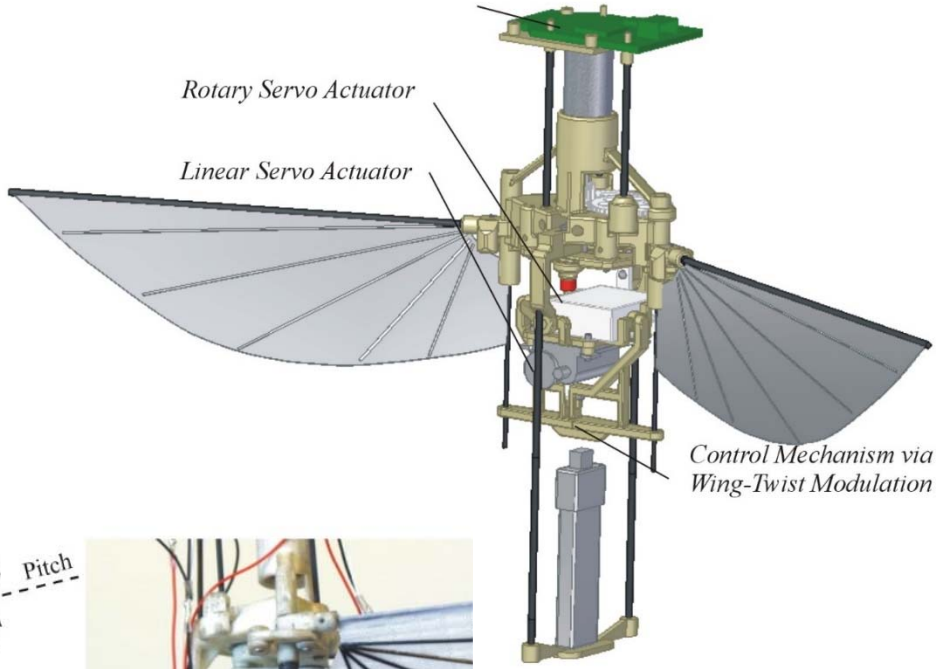

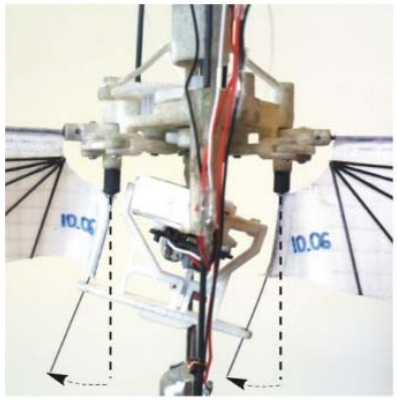

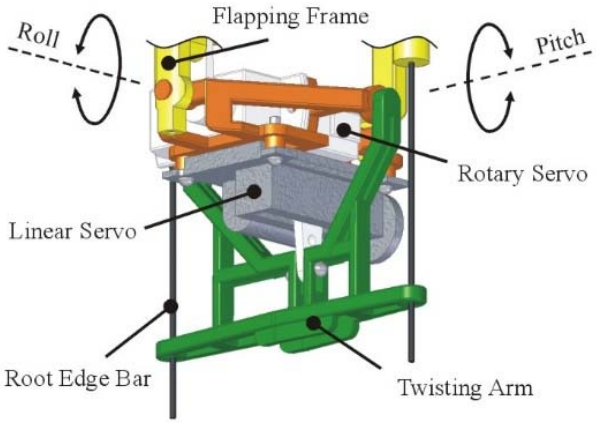

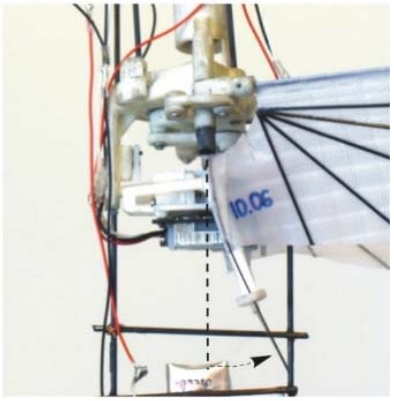

Control bars actuation for generating Pitch-Roll-Yaw moments

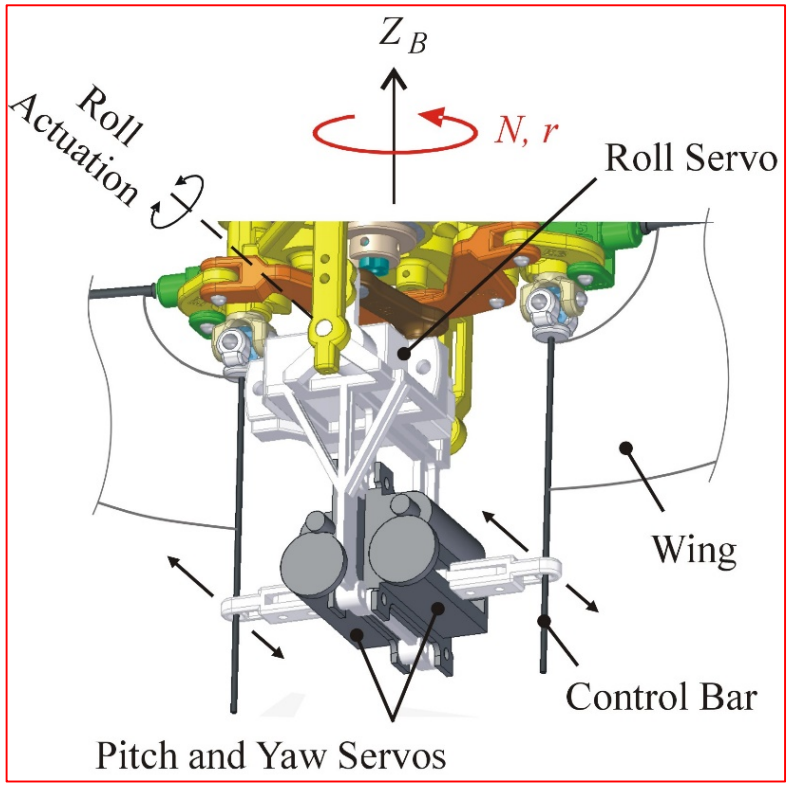

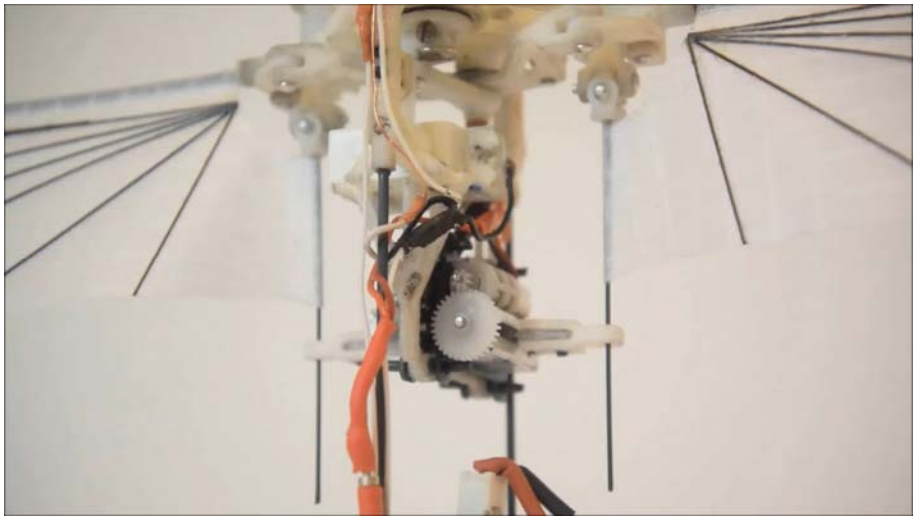

Experimental setup
For the measurement
of the control moments

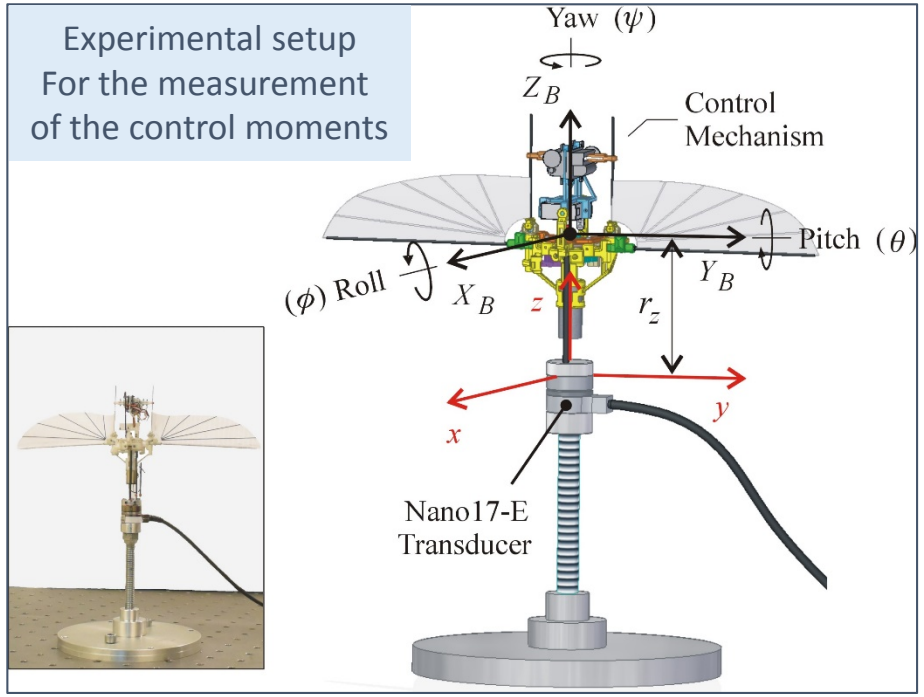

The **lift** and the **roll** and **pitch** control moments are nearly decoupled

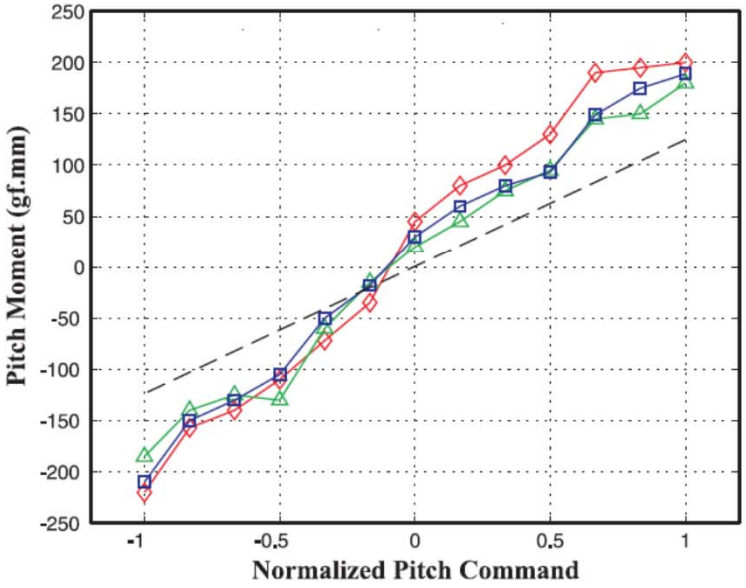

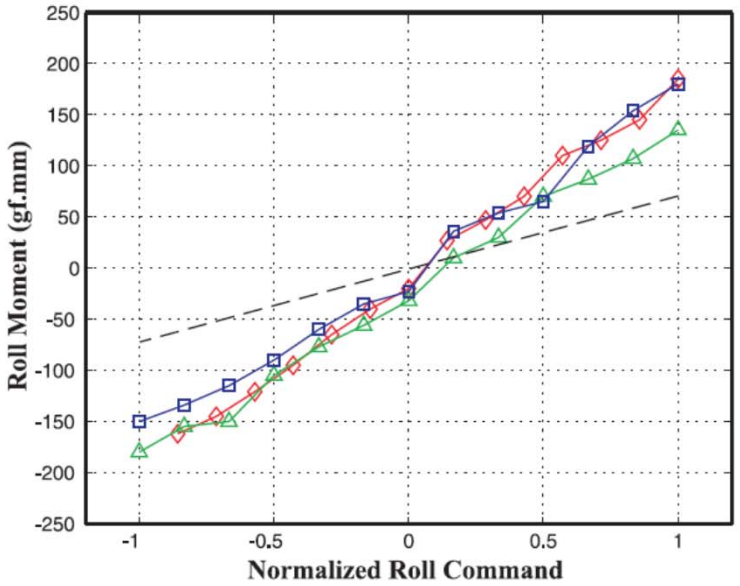

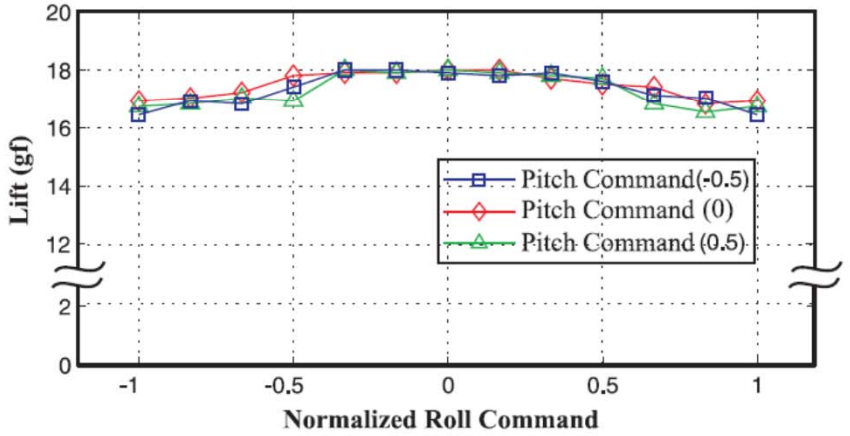

Dynamics and control

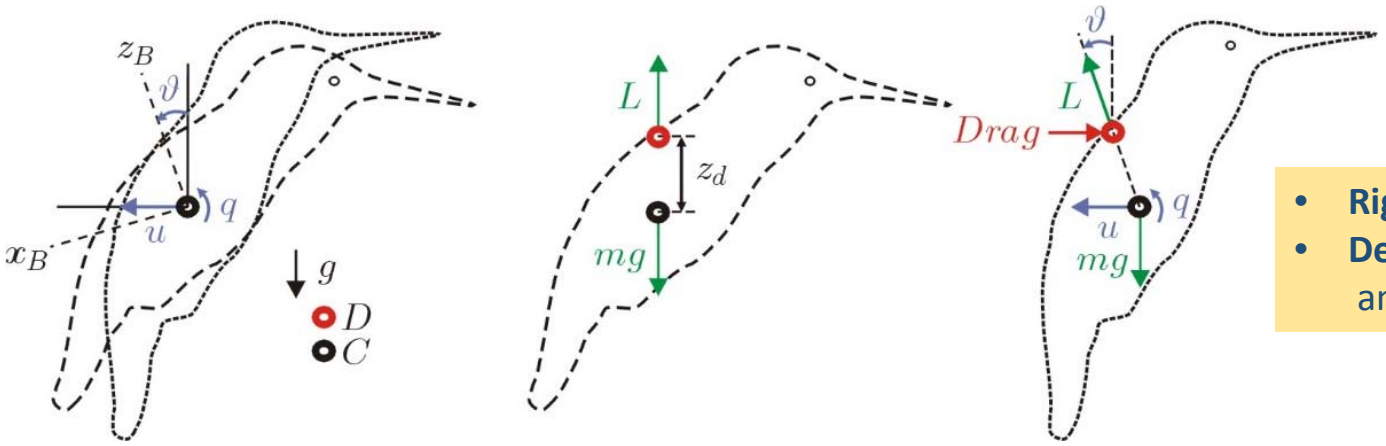

- **Rigid body dynamics**
- **Decoupling** longitudinal (pitch) and lateral (roll) dynamics

Longitudinal dynamics:

Newton:

$$m\dot{u} = X_u u + X_q q + mg\theta$$

Euler:

$$I\dot{q} = M_u u + M_q q + \tau$$

$$\begin{Bmatrix} \dot{u} \\ \dot{q} \\ \dot{\theta} \end{Bmatrix} = \begin{bmatrix} \hat{X}_u & \hat{X}_q & g \\ \hat{M}_u & \hat{M}_q & 0 \\ 0 & 1 & 0 \end{bmatrix} \begin{Bmatrix} u \\ q \\ \theta \end{Bmatrix} + \begin{Bmatrix} 0 \\ 1 \\ 0 \end{Bmatrix} \frac{\tau}{I_{yy}}$$

Control torque

Damping mechanism

- The dominant damping mechanism is the wing motion
- The wing velocity *w* is such that *w>>u*
- The drag forces are linear in the robot velocity *u*

$$f_d = -\beta(w+u)^2 + \beta(w-u)^2 = -4\beta w u = -K u$$

$$f_d = -K(u + q\, z_d)$$

Linear velocity of the center of drag

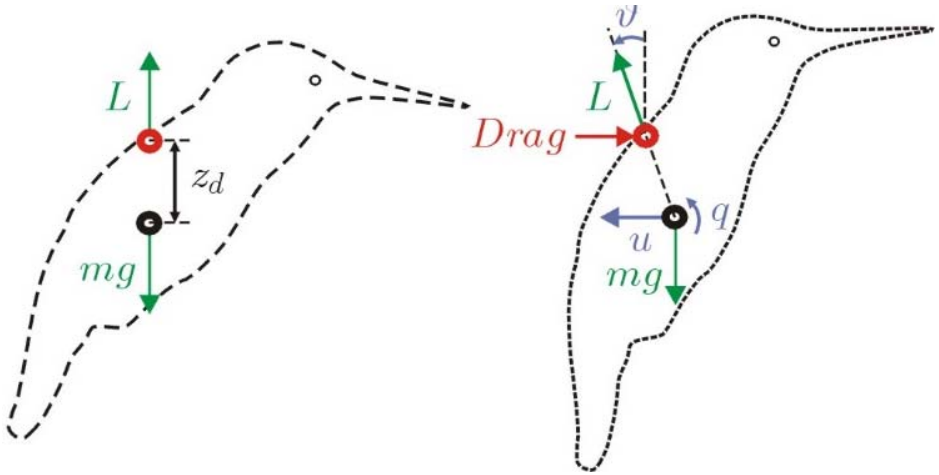

Newton:

$$m\dot{u} = X_u u + X_q q + mg\theta$$

Euler:

$$I\dot{q} = M_u u + M_q q + \tau$$

Experimental set-up for determining X_u

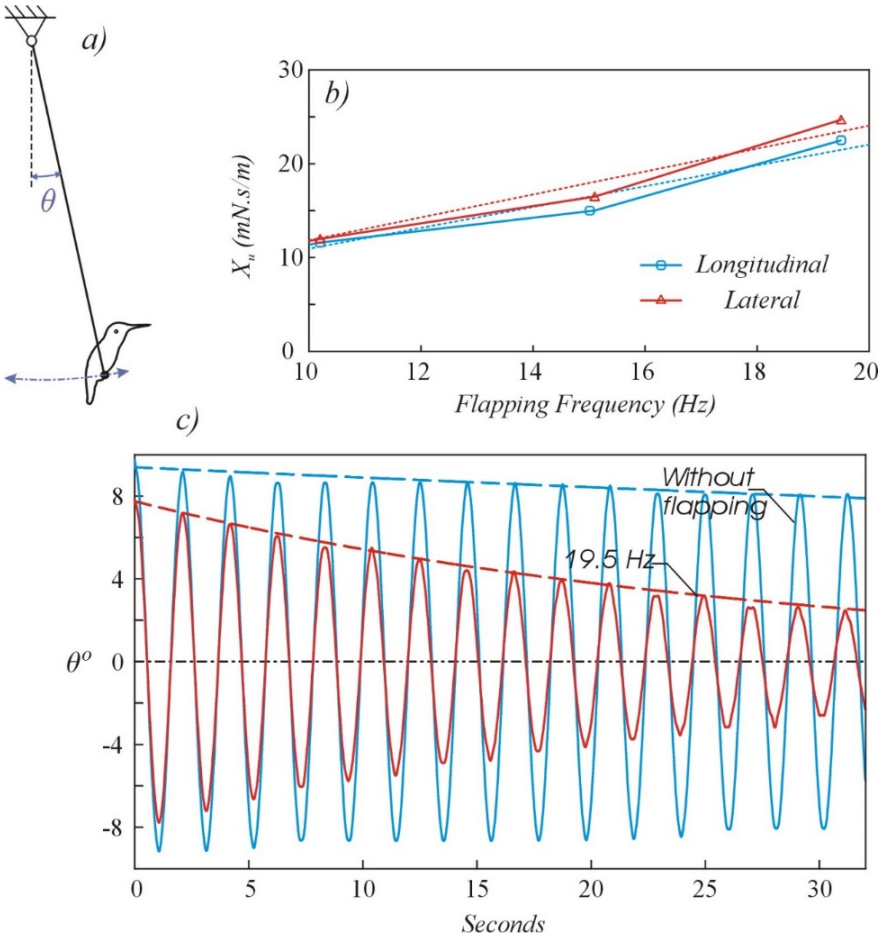

Experimental set-up for determining M_q

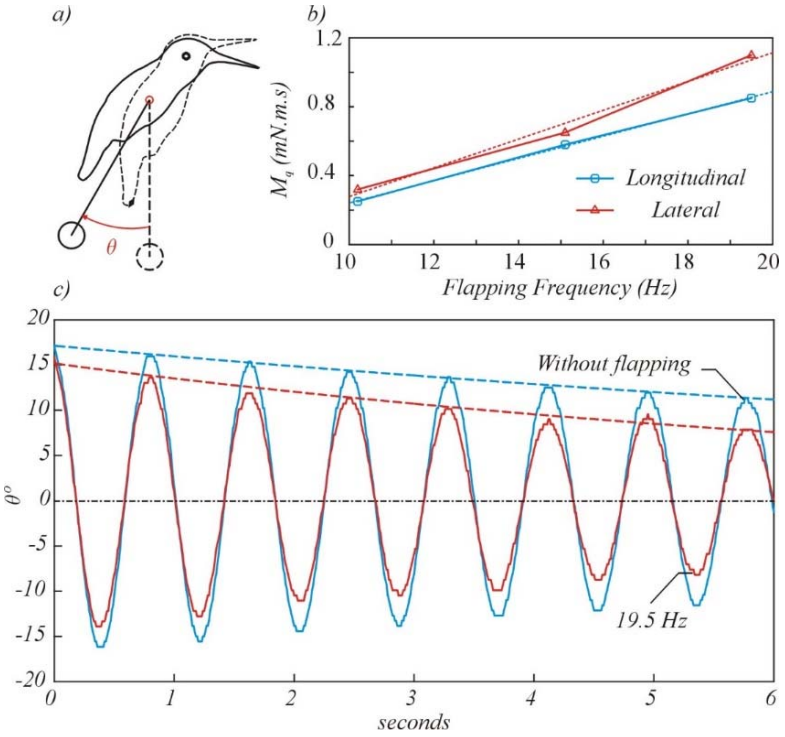

Open-loop dynamics

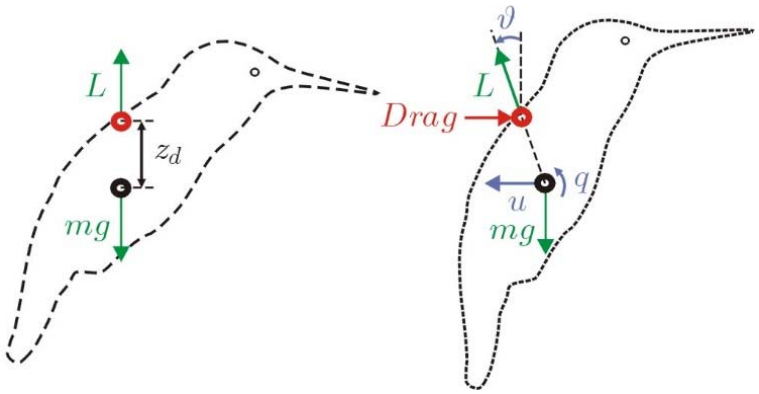

Always negative

Negative if $z_d>0$
Positive if $z_d<0$

$$\begin{Bmatrix} \dot{u} \\ \dot{q} \\ \dot{\theta} \end{Bmatrix} = \begin{bmatrix} \hat{X}_u & \hat{X}_q & g \\ \hat{M}_u & \hat{M}_q & 0 \\ 0 & 1 & 0 \end{bmatrix} \begin{Bmatrix} u \\ q \\ \theta \end{Bmatrix}$$

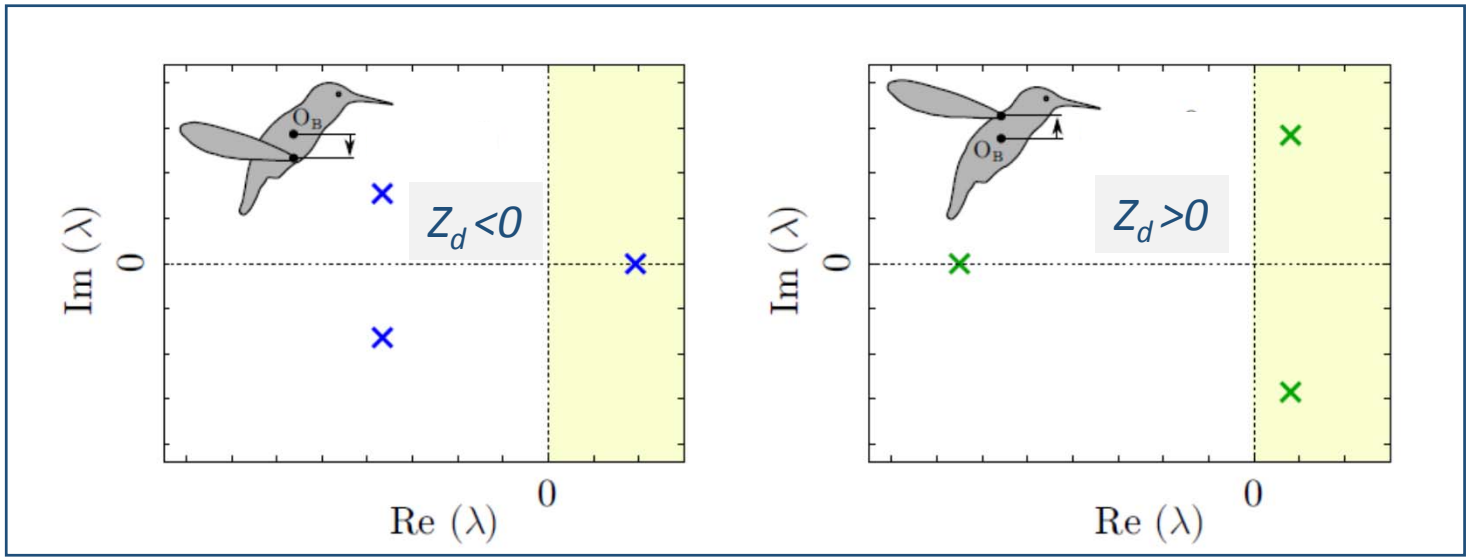

Closed-loop dynamics

$$\tau / I_{yy} = -k_\theta \theta - k_q q$$

Actuator dynamics:
time constant T of 80 ms on the roll axis
and 100 ms on the pitch axis

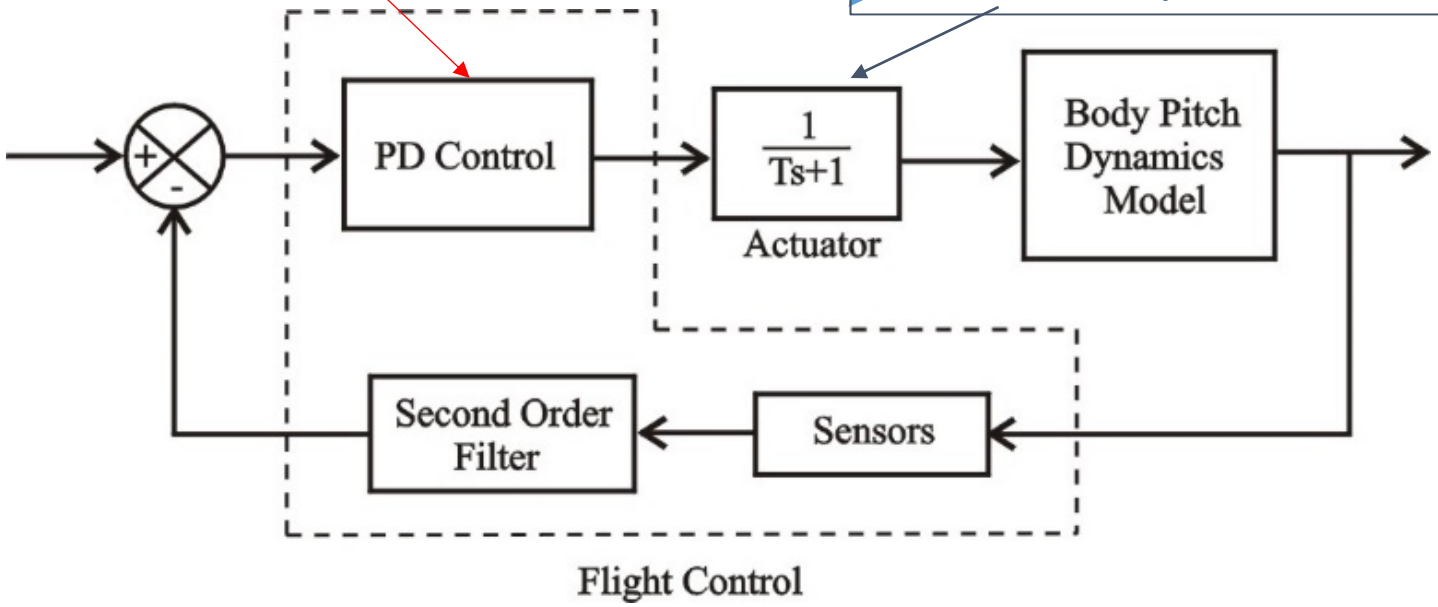

Closed-loop dynamics

$$\begin{Bmatrix} \dot{u} \\ \dot{q} \\ \dot{\theta} \\ \dot{\tau}_a \end{Bmatrix} = \begin{bmatrix} \hat{X}_u & \hat{X}_q & g & 0 \\ \hat{M}_u & \hat{M}_q & 0 & 1 \\ 0 & 1 & 0 & 0 \\ 0 & -k_q/T & -k_\theta/T & -1/T \end{bmatrix} \begin{Bmatrix} u \\ q \\ \theta \\ \tau_a \end{Bmatrix}$$

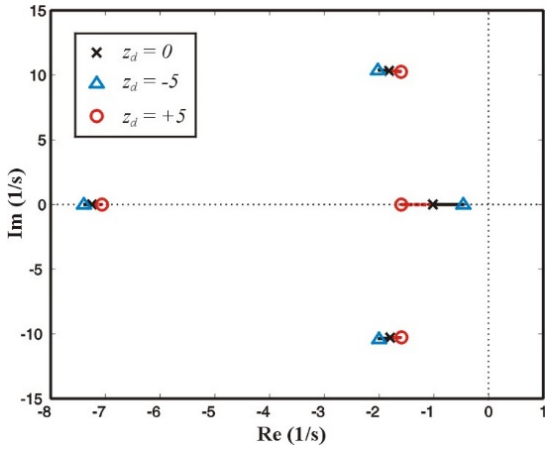

Sensitivity of the closed-loop poles to the position of the center of drag.

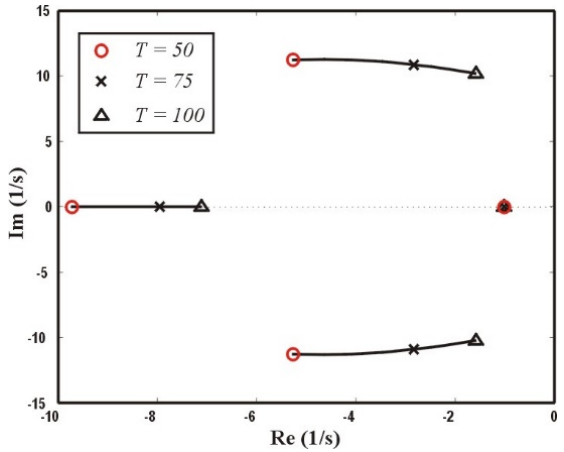

Sensitivity of the closed-loop poles To the time constant of the attitude Control actuator.

First flights with sails (no control)

Depending of sail configuration

- Oscillatory instability
- Divergent instability
- Stable flight

$$\begin{Bmatrix} \dot{u} \\ \dot{q} \\ \dot{\theta} \end{Bmatrix} = \begin{bmatrix} \hat{X}_u & \hat{X}_q & g \\ \hat{M}_u & \hat{M}_q & 0 \\ 0 & 1 & 0 \end{bmatrix} \begin{Bmatrix} u \\ q \\ \theta \end{Bmatrix}$$

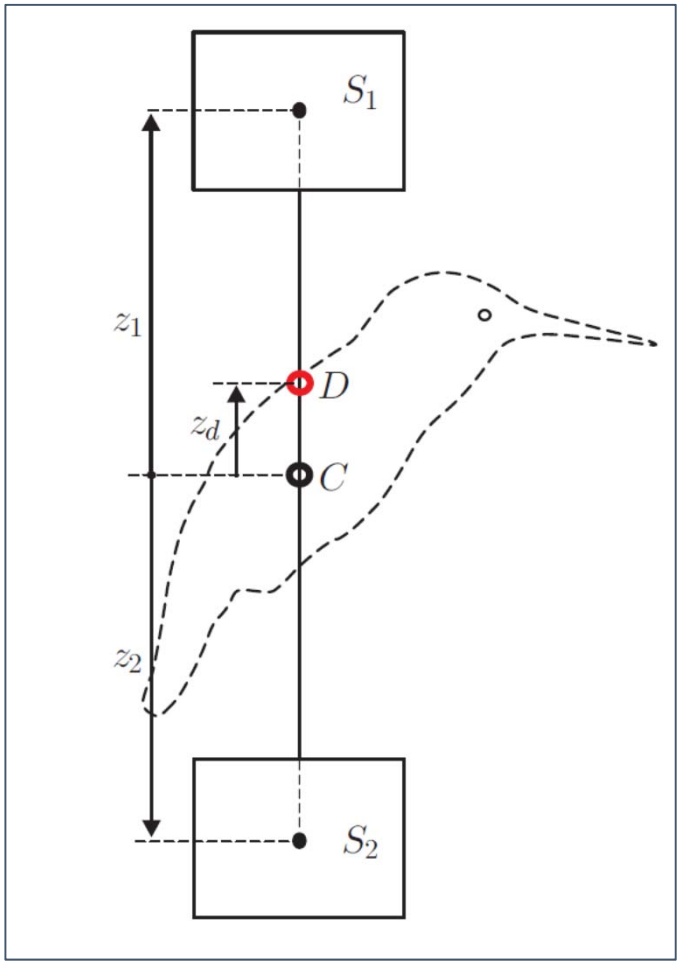

Flight with sails

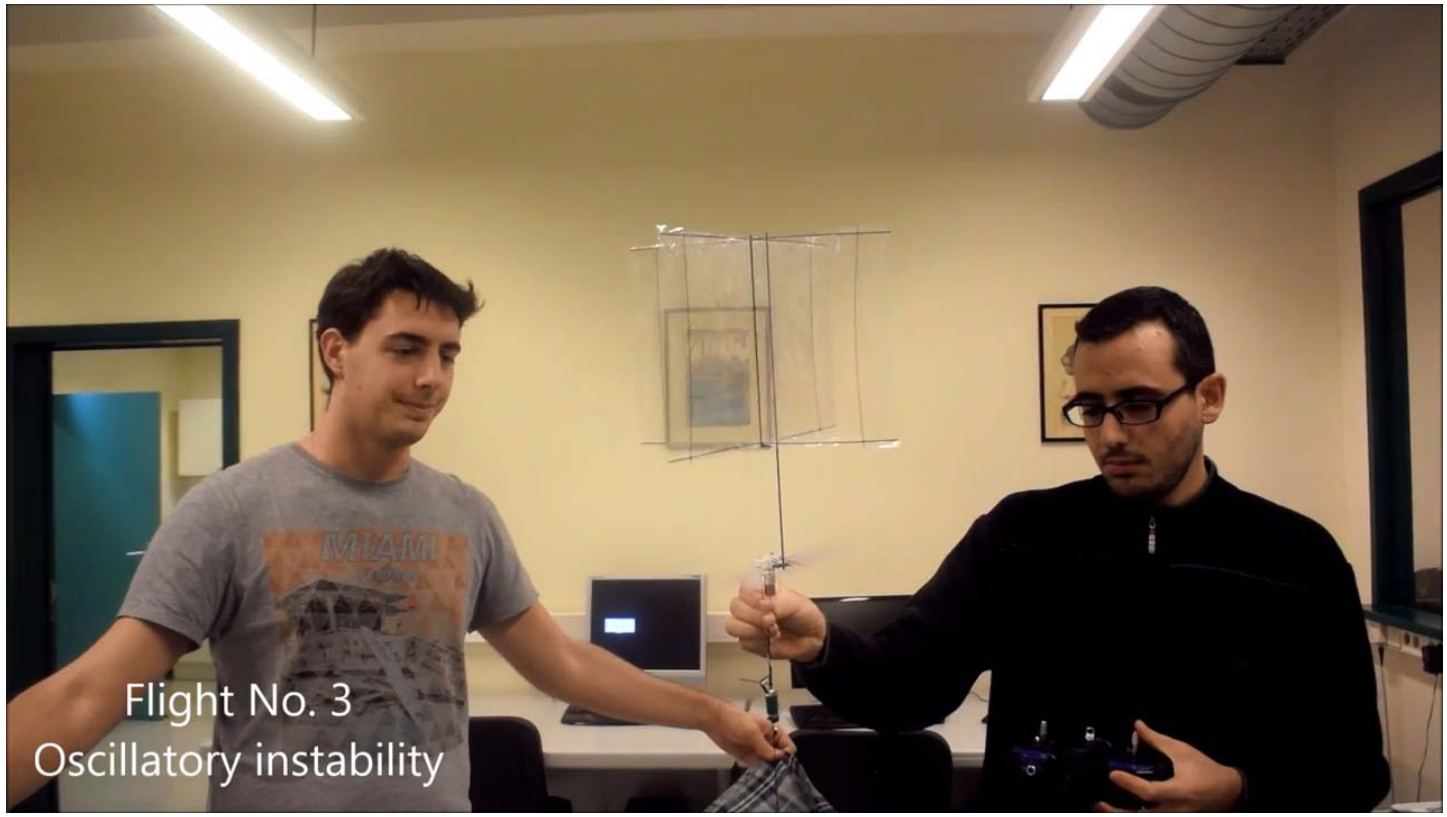

Maiden flight (June 23, 2016)

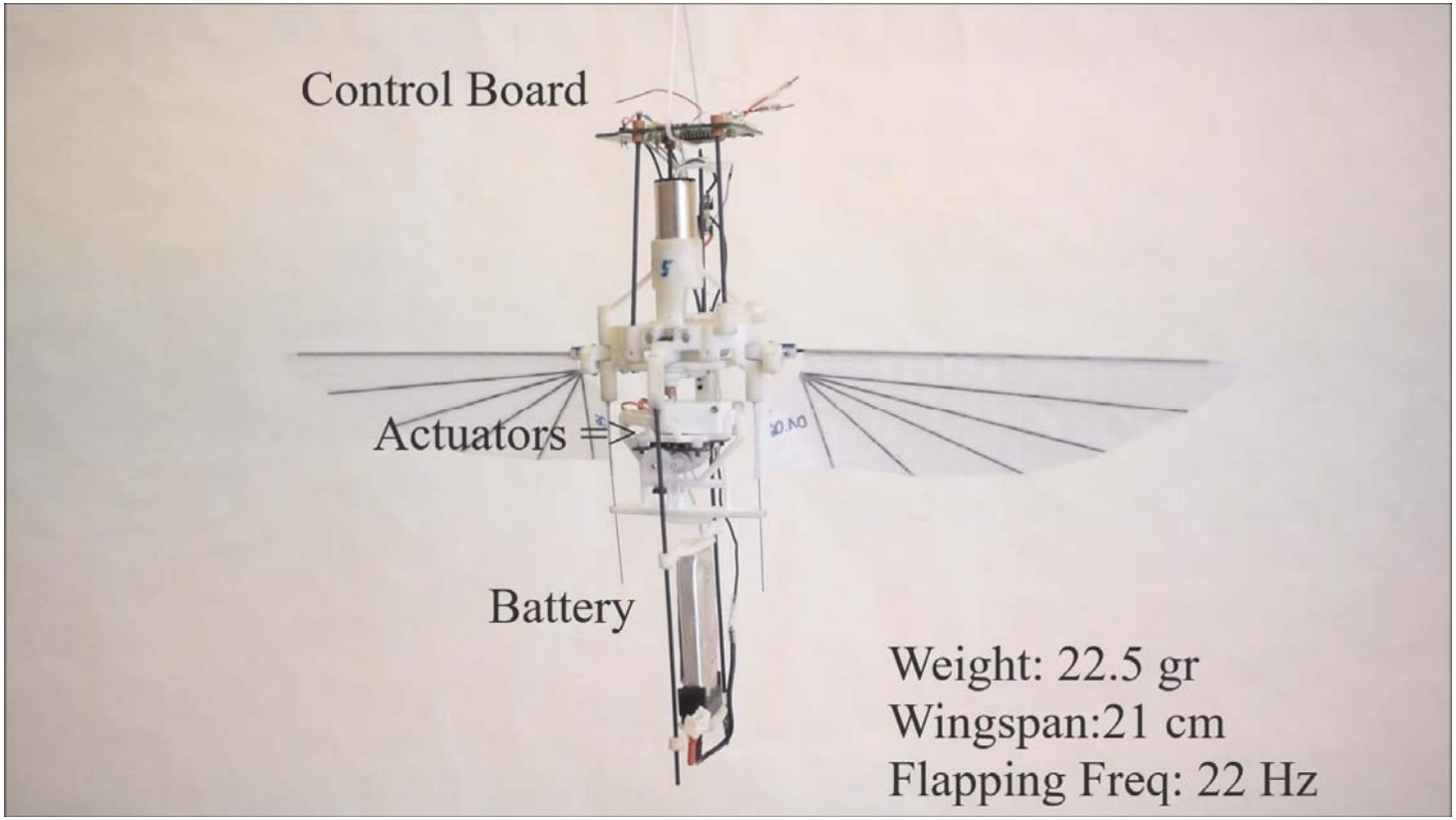

Cascade control structure for the axial dynamics

The inner loop control the pitch attitude

The outer loop control the drift speed

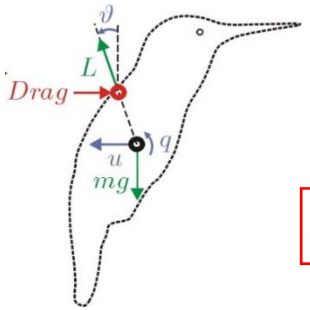

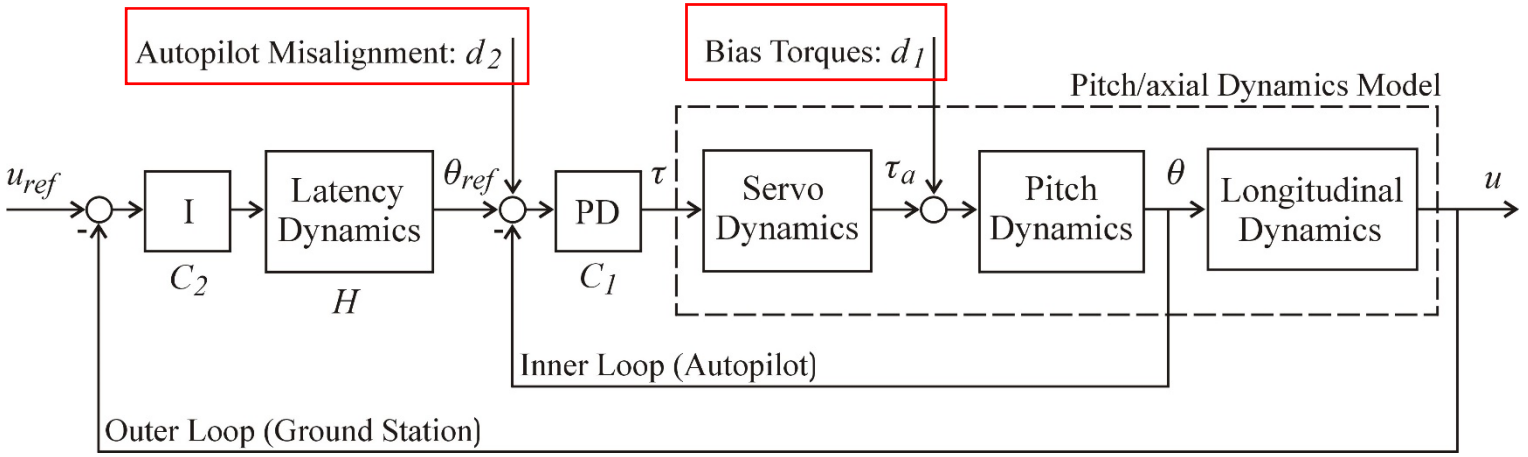

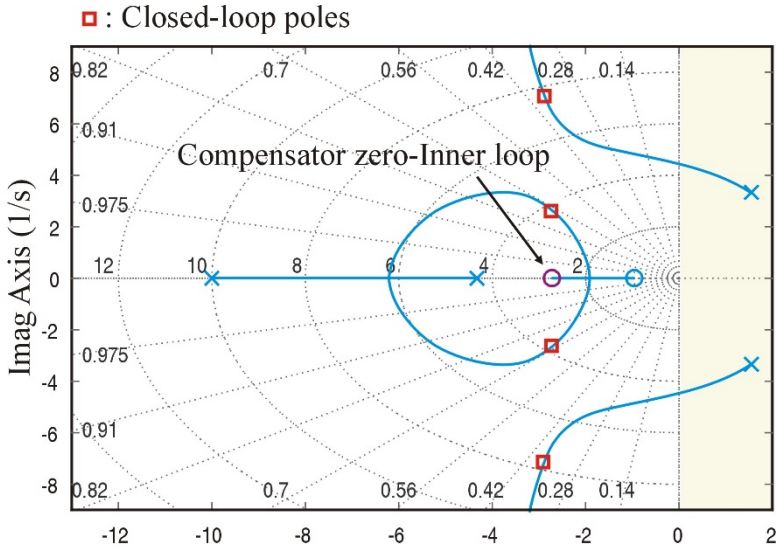

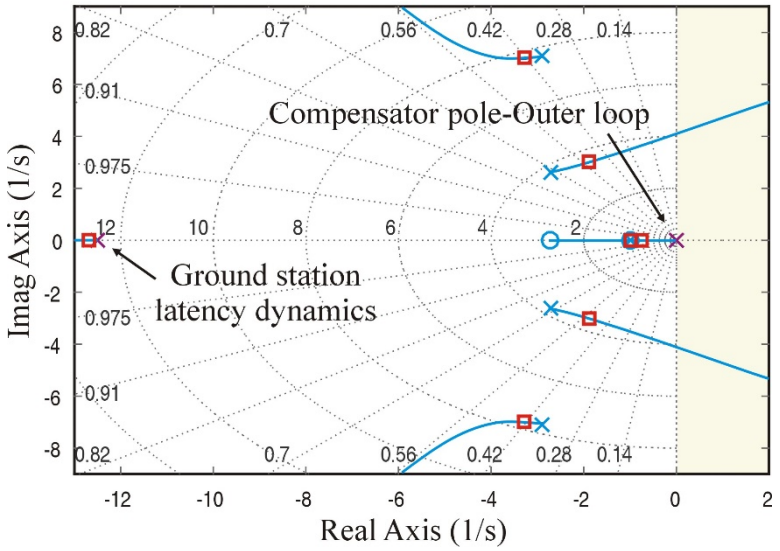

X-Y trajectory during flight tests

Red: PD control (inner loop)

Green: Cascade control (outer loop)

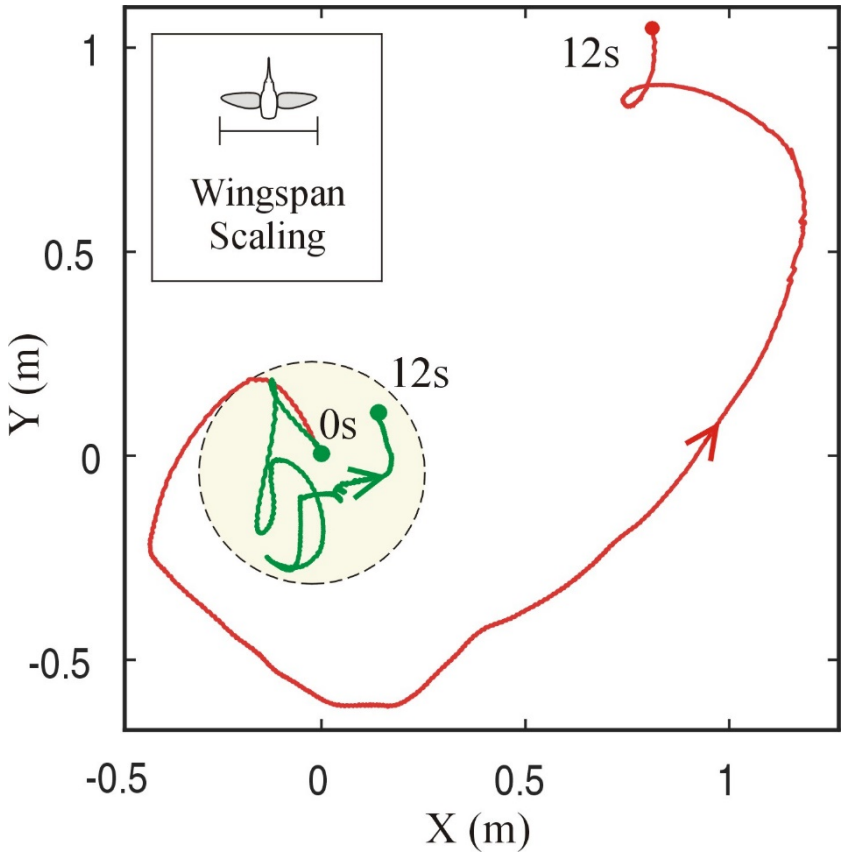

Take-off and drift speed control via cascade controller

(slow motion x 0.5)

Weight distribution

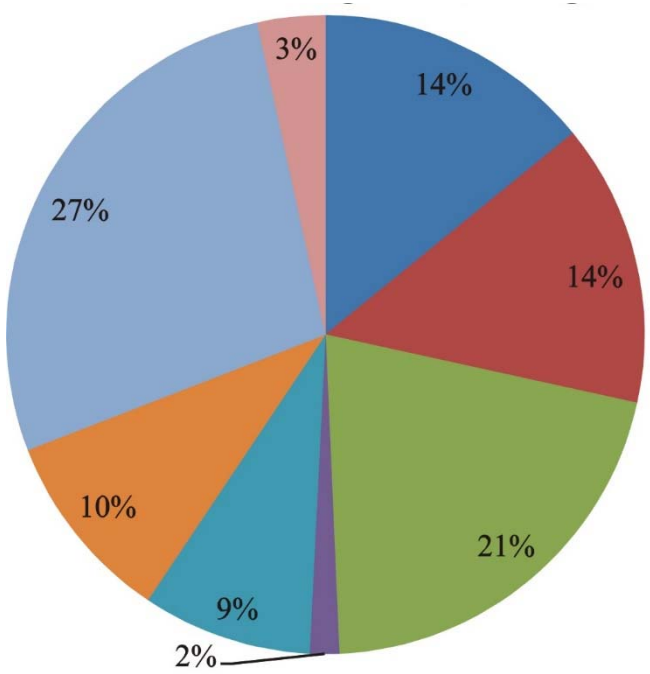

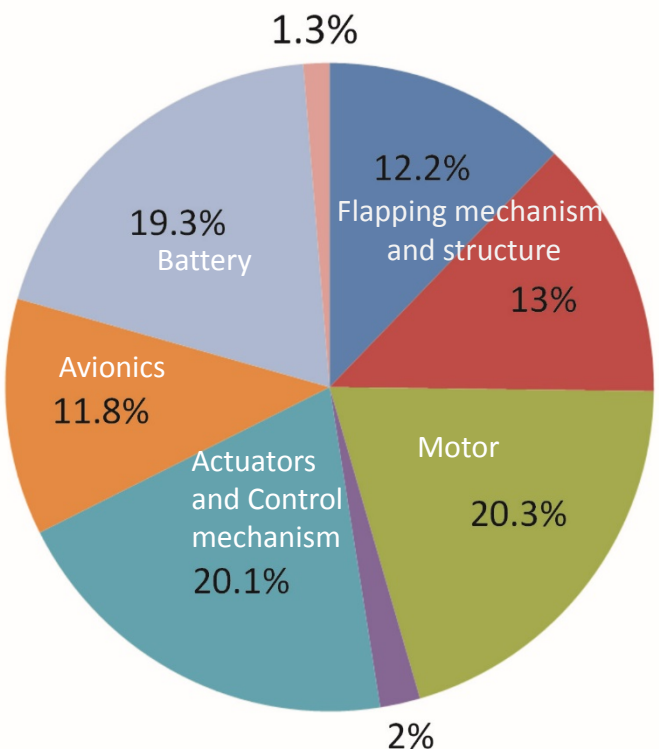

Darpa-AeroVironment Nano-hummingbird 19 gr

- *Flapping mechanism*
- *Structure*
- *Driving motor*
- *Wings*
- *Control mechanism*
- *Avionics*
- *Battery*
- *Wiring*

Colibri robot 23.85 gr

Future work

- Improving **motor efficiency** by changing the operating point
  (currently, the flight time is limited by the thermal limit of the motor)
- Redesign of the pitch-roll-yaw **actuators**
  (lighter, faster, more stroke)
- Implementing cascade control from **on-board data**
  (use GPS instead of tracking cameras to implement the cascade control)
- Pursue the **aeroelastic** study to improve **lift and aerodynamic efficiency**
- **Weight**, weight, weight….

Thank you !